

Simulation driven design of timber bolster in fibre composite

MARCUS RIBBENSTEDT
NICK SALAVATI

marrib@kth.se
nicks@kth.se



Master of Science Thesis
Stockholm, Sweden 2016

Abstract

The primary objective of this thesis is to investigate a simulation and optimisation based methodology using fibre composite materials to lower the weight of timber bolsters. The timber bolsters secure the timber from falling off the truck during loading and transport. A lighter forestry truck is beneficial for several reasons such as increased payload and fuel efficiency and a decreased environmental impact.

This thesis includes a concept study for a bolster made of fibre composites. Carbon and glass fibres together with polyurethane were chosen as material system and the recommended manufacturing methods were pultrusion and resin transfer moulding. A study of the economy related to the timber transport was conducted during the concept phase to investigate the potential business case.

The thesis also includes an optimisation of the generated concept. The optimisation focused on geometry and fibre layup. By the use of optimisation the weight was reduced from the initial 136 kg of aluminium to 87 kg of glass and carbon fibre. The optimised design was compared with today's aluminium bolsters and indicated that the composite bolster is realistic from an economic perspective.

A methodology for analysing bolted joints in fibre composites was developed. The analysis was made using the finite element method and resulted in a comparison between different failure criteria. Based on the results it can be concluded that the prediction of failure differs significantly depending on used failure criterion and tests are needed for verification.

Finally a simulation was made to verify the structures response to an impact. The simulation was compared with calculations using energy equations showing a fairly good agreement.

Sammanfattning

Det huvudsakliga syftet med detta examensarbete var att använda metodik baserad på simulering och optimering samt fiberkompositmaterial för att minska vikten på timmerbankar. Timmerbankar används för att lastsäkra timmer på lastbilar under lastning och transport. En lättare lastbil är fördelaktig av flera anledningar som t.ex. ökad kapacitet för nyttolast och bränsleeffektivitet samt en minskad miljöpåverkan.

Examensarbetet inkluderar en konceptstudie för en timmerbanke i fiberkomposit. Kolfiber och glasfiber tillsammans med polyuretan valdes som material. Pultrusion och resin transfer moulding rekommenderades som tillverkningsmetoder. En studie av ekonomin relaterad till timmertransport genomfördes under konceptstudien för att undersöka om konceptet har potential att vara ekonomiskt gångbart.

Examensarbetet innehåller även en optimering av det genererade konceptet. Optimeringen fokuserade på geometri samt kompositlaminatets fiberriktningar och stackningsordning. Genom användning av optimering minskades vikten på banken från dagens 136 kg i aluminium till 87 kg med glas och kolfiber. Den optimerade banken jämfördes med en existerande aluminiumbanke ur ett ekonomiskt perspektiv och slutsatsen är att med de givna antagandena har den optimerade konstruktionen större ekonomisk potential.

En metod för att analysera skruvförband i komposit utvecklades och olika brottkriterier har undersökts. Analysen genomfördes med finita elementmetoden och resulterade i en jämförelse mellan olika brottkriterier. Baserat på resultaten kan det konstateras att prediktering av brott påverkas avsevärt av använt brottkriterium och att verifierande provning behövs.

Slutligen genomfördes en simulering för att verifiera strukturens respons vid en slag last. Simuleringen jämfördes med beräkningar baserade på energiekvationer och på påvisade skaplig överensstämmelse.

Preface

This master thesis finalises our studies at the Royal Institute of Technology's (KTH) vehicle engineering program. This work also ends our studies at the Master of Science in Aerospace Engineering programme at KTH.

This thesis was carried out at Scania's department for Dynamics and Strength analysis (RTCC) and we would like to thank our colleagues for meaningful and interesting discussions and support.

We would like to highly acknowledge our supervisor Andreas Rietz for his huge effort to support and guide us through this work.

Our supervisors Niklas Edrén from Altair deserves special recognition for his efforts and helpful advice regarding modelling.

We would also like to mention our appreciations to Dan Jönsson for his valuable input, Marstrom Composite AB for their technical advice and our academic supervisor Magnus Burman for his guidance throughout the work.

Table of Contents

Nomenclature	1
1. Introduction	3
1.1 Objective.....	3
1.2 Timber transports in general.....	3
1.3 Existing lightweight timber bolster	3
1.4 Division of work	4
1.5 Used software	4
2. Product functionality and requirements	5
2.1 Bolster for comparison	5
2.2 Specification of requirements	5
2.3 Origin of loads and requirements	8
3. Conceptual study	10
3.1 Global geometry concepts	10
3.2 Cross sections	12
3.3 Manufacturing	13
3.4 Fibre materials	14
3.5 Matrix materials.....	15
3.6 Conceptual design summary.....	16
3.7 External feedback	17
4. Business case for composite bolster.....	18
5. Modelling methodology	21
5.1 Prepare CAD model.....	21
5.2 Generate mesh	21
5.3 Create laminate	21
5.4 Composite alignment.....	22
6. Optimisation of fibre composite timber bolster	23
6.1 Optimisation methodology	23
6.2 Analysis setup.....	29
6.3 Results	31
6.4 Discussion of optimisation procedure	34
6.5 Conclusions of optimisation	35
7. Joints in composite structures	36
7.1 Joining techniques	36
7.2 Failure modes in bolted laminates	37
7.3 Design guidelines	39
7.4 Modelling of bolted joints	41

7.5	Failure analysis in composites	46
7.6	Results	52
7.7	Discussion of bolted joint analysis	55
7.8	Conclusions of bolted joint analysis	57
8.	Impact analysis	58
8.1	Method	58
8.2	Results	59
8.3	Discussion of impact analysis	60
9.	Concluding remarks	61
	References	62
	Appendix A. Fatigue of fibre composites	66
	Appendix B. Material properties	67
	Appendix C. Rubber epoxy	67
	Appendix D. Optimisation layup of non-design space	68
	Appendix E. Optimised ply shapes	69
	Appendix F. Maximum strain variation	70
	Appendix G. Abaqus UMAT subroutine	71

Nomenclature

The used nomenclature is displayed in Table 0.1 below where $i = 1, 2, 3$ are according to the directions defined in Figure 0.1. Furthermore the 0° fibre orientation is defined in Figure 0.2 which also includes a global coordinate system.

Table 0.1: *Used nomenclature in the report.*

Notation	Description	Unit
E_i	Young's modulus in direction i	Pa
f_1	Lowest natural frequency while driving empty	Hz
G_{12}	Shear modulus in 1-2 plane	Pa
m	Mass	kg
t	Laminate thickness	m
u	Displacement at the top of the bolster	m
v	Speed	m/s
$\hat{\epsilon}_{it}$	Strain limit in tension in direction i	-
$\hat{\epsilon}_{ic}$	Compressive strain limit in direction i	-
$\hat{\gamma}_{ij}$	Shear strain limit in i - j plane	-
ρ	Density	kg/m ³
$\hat{\sigma}_{it}$	Stress limit in tension in direction i	Pa
$\hat{\sigma}_{ic}$	Compressive stress limit in direction i	Pa
$\hat{\tau}_{ij}$	Shear stress limit in i - j plane	Pa

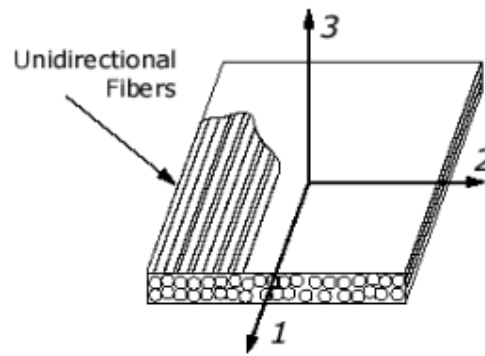


Figure 0.1: *Local coordinate system aligned with fibre direction [1].*

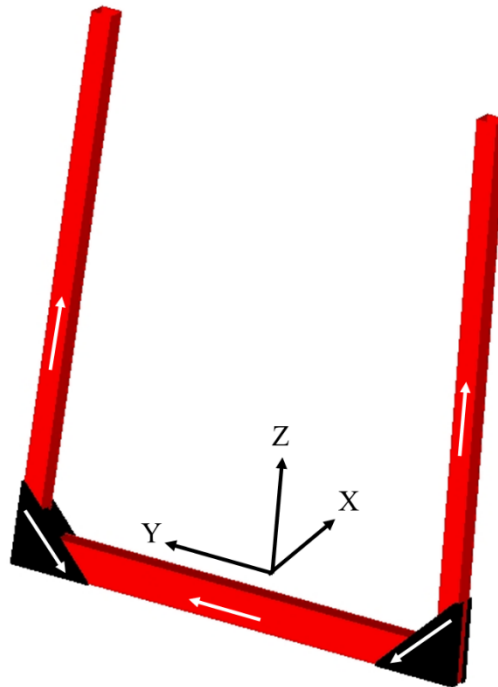


Figure 0.2: *Coordinate system and white arrows defining the 0° fibre orientations.*

1. Introduction

1.1 Objective

The main objective of this thesis is to study simulation and optimisation driven design of a composite component. More precisely the objective is to use simulation driven design and optimisation to lower the weight of a timber bolster. Furthermore an increased understanding of simulation driven design and a modelling methodology for bolted joints in composites is of interest. The approach is to serve as a reference demonstrating the potential with using composite materials and optimisation.

1.2 Timber transports in general

Decreased fuel consumption and lower CO₂ emissions from timber transports has been considered in earlier studies, for example the Skogsforsk project “ETT-Modulsystem för skogstransporter” [2]. The timber transport industry often runs heavily loaded and therefore the need to save weight is high. The timber industry has increased its efficiency the past years by decreasing the number of saw mills leading to longer transport distances [2]. This further motivates the work to achieve lighter trucks. Moreover the industry had a turnover of approximately 4 billion kr in 2010 [3] making it important for the Swedish economy.

1.3 Existing lightweight timber bolster

Composite materials have been used in timber transport vehicles before by for example Deloupe Inc. in Canada. The bolster developed for the forestry vehicle was part of a public research project. Composite material was used for the vertical and horizontal beams of the timber bolster, seen in grey in Figure 1.1.



Figure 1.1: *Timber transport using grey coloured fibre composite beams [4].*

The green corners in Figure 1.1 were made of steel and supports the structure to avoid large displacements at the top of the bolsters when loaded. The composite of choice was the Baydur PUL 2500 resin with glass fibres [5, 6]. Significant amount of research was done to design the

matrix to be suitable for mass production. Especially the elongation to failure and impact resistance was of interest due to the harsh environment when loading timber trailers [6]. As an example the weight percentage of glass fibre could be 80 % [5]. As noted by Vaillancourt [7] the cost increased by 20% but the weight was decreased by approximately 40%. According to Jacob [8] the approximate weight of each bolster is 90 kg. There are however several unknown parameters to consider regarding the weight data. The extent of the bolsters integration to the chassis is unknown, making it difficult to predict weight saving of the bolster alone and not the total weight saving. The loads that the bolster has been designed for and the stiffness requirements are also unknown, however the mechanical properties were tested with both static and dynamic loads [6]. Customer tests have also been done by using the bolsters in the timber transport industry.

1.4 Division of work

The authors worked together with chapters 1-5 and 9. Marcus Ribbenstedt worked with chapters 6 and 8 regarding optimisation and impact analysis and Nick Salavati worked with chapter 7 concerning bolted joints.

1.5 Used software

The following software were used in the project:

- CATIA V5 - CAD program used to generate geometry.
- Hypermesh 14.0 - Pre-processing tool used for geometry clean up and meshing.
- Optistruct 14.0 - FE-solver used for structural optimisation and analysis.
- Hyperview 14.0 - Post-processing tool used to analyse results from FE-simulations.
- Abaqus implicit 6.14 - Implicit FE-solver.
- Abaqus explicit 6.14 - Explicit FE-solver used for impact analysis.
- Abaqus viewer 6.14 - Post-processing tool used to analyse results from FE-simulations.

2. Product functionality and requirements

This section describes a product currently on the market which is to be used as a reference. The specification of requirements is also included in this section.

2.1 Bolster for comparison

The bolster designed within this thesis will be compared with an existing timber bolster made of aluminium. One of the world leading timber bolster manufacturer Exte produces a 136 kg aluminium bolster named A10 [9]. This bolster is visualised in Figure 2.1.

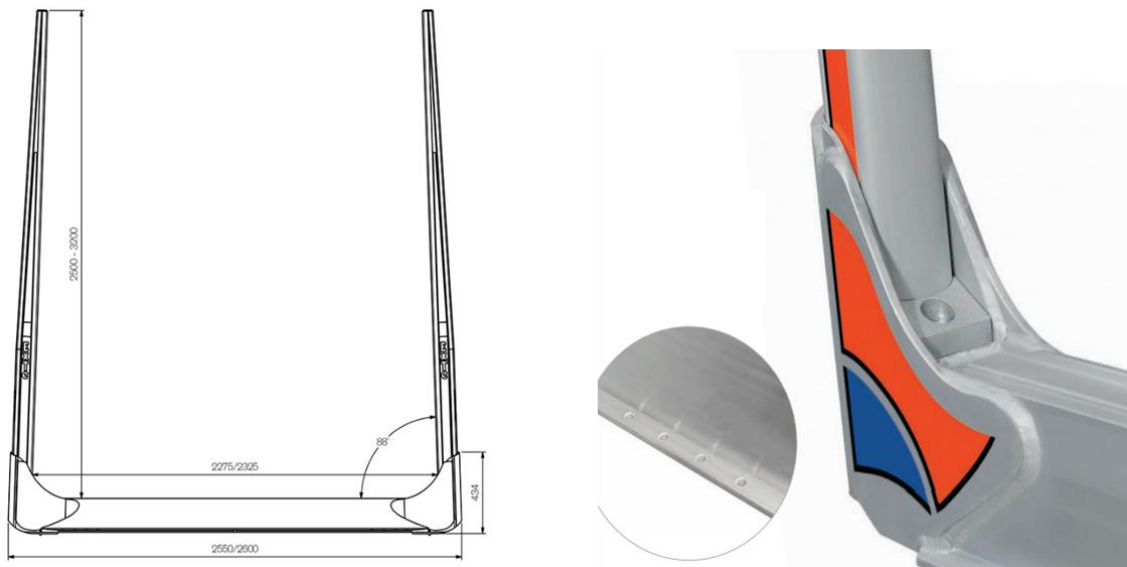


Figure 2.1: A10 aluminium bolster from Exte [10].

As seen in Figure 2.1 the vertical beams are tapered and the corners are reinforced to withstand the loads. The A10 bolster was chosen as comparison since it is a product that focus on lightweight and is part of Exte's lightweight series.

The comparison will be made against the aluminium bolster since it's a commercial product proven to work in the transport industry. The aluminium bolster is mounted onto a standardised auxiliary frame in contrast to the existing fibre composite bolster described in Section 1.3. This further indicates that the aluminium bolster is the most relevant bolster for comparison.

2.2 Specification of requirements

A timber bolster is mounted on the auxiliary frame of a truck. The purpose is to fasten and secure the timber for long distance transportation. In Table 2.1 the various requirements of the timber bolster are specified. These requirements include structural demands, material selection, environmental demands, maintenance and the positioning of the bolster in order to obtain a detailed view of the various demands on the product. In Table 2.1 the type of demands are divided into primary (P) and additional (A) demands. Primary demands have been considered and evaluated whereas additional demands have not been

prioritised or specifically considered within this thesis. More details regarding the origin of the loads can be found in Section 2.3.

Table 2.1: *Specification of requirements.*

Demand	Specification	Type of demand
Materials		
	Materials should not be listed in Scania <ul style="list-style-type: none"> • black (STD4158) or • grey (STD4159) list considering health and environmental aspects	A
	Material should withstand precipitation	A
	Tolerate temperatures between -40 to 100°C	A
	Surface treatment according to Scania STD4111	A
	Flame spreading of maximum 75 mm/min	A
	The bolster must be fire resistant according to the standard FMVSS 302 and the technically equivalent ISO 3795 (Europe)	A
	No corrosion is to occur in road environment	A
Dimensions		
	Maximum height 3 m and maximum width 2.55 m, see Figure 2.2	P
Manufacturing volume		
	1000 units/year	P
Structural		
Fatigue loads (1 000 000 cycles)	0.3g · 10 tonnes horizontally, y-direction	P
	10g acceleration in x, y, z-directions	P
	3g · 10 tonnes vertical load	P
Maximum load	0.5g · 10 tonnes horizontally, y-direction	P
Stiffness	Displacement $u < 35$ cm	P

Impact load	190 kg log moving at 2 m/s, see Figure 2.4	A
Dynamics	Lowest natural frequency $f_1 > 7$ Hz	P
Strength	Safety factor 3 against failure from fatigue loads, see Appendix A	P
	Safety factor 1 against failure for maximum load	P
Buckling	Buckling safety factor > 1	P
Abrasion	Withstand fretting from timber	P
Unnotched laminate guidelines		
	Laminate layup should consist of 0° , 45° , -45° and 90° oriented plies	P
	Laminate layup should be symmetrical and balanced	P
	Laminates should have at least 5 % of their plies in each direction	P
	Laminates should consist of max 70 % of plies in any direction	P
	Maximum 3 plies (0.75 mm) of any fibre orientation stacked adjacent to each other	P
Notched laminates		
	Laminates should consist of max 60 % of plies in any direction	P
	Bolted joints should not have less than 35 % of plies in $\pm 45^\circ$	P
Delimitations of project		
	The auxiliary frame is not to be included in the analyses	P
	The logs are assumed to act as evenly distributed loads during vehicle operation	P
	The bolster is to be mounted on a standardised Scania truck and must therefore have mounts that corresponds to the existing framework for Scania's standardised auxiliary frame	A

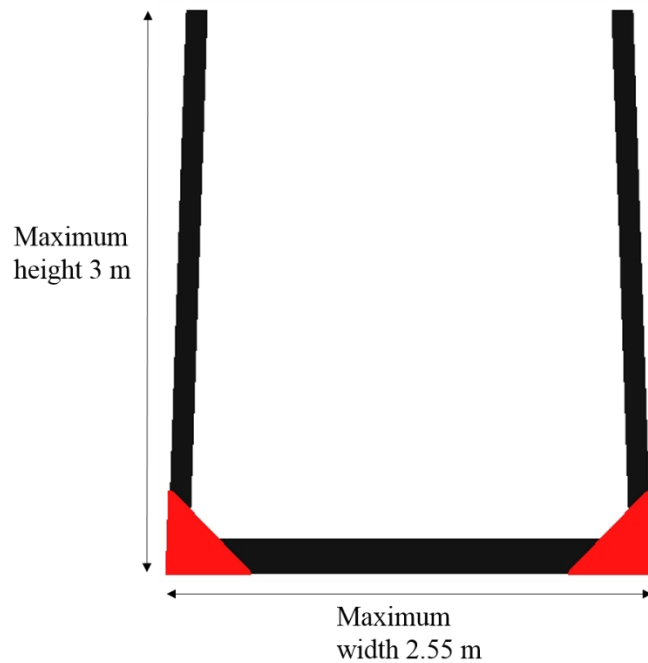


Figure 2.2: *Maximum dimensions for the timber bolster.*

2.3 Origin of loads and requirements

The maximum load the truck should handle laterally before rolling over sideways is $0.5g$. This demand is stated by the Swedish Transport Administration [11] and can be seen in Figure 2.3 below.

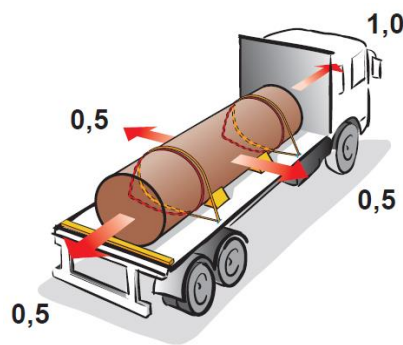


Figure 2.3: *Illustration of g-force load requirements [12].*

Similarly the timber bolster is subjected to a lateral load of $0.3g \cdot 10$ tonnes when the truck is turning at relatively high speeds. Typically the truck is subjected to an acceleration of $0.3g$ when entering or exiting a highway.

When transporting a full set of timber and driving over a bump a vertical acceleration implies loads on the timber bolster. This vertical load is applied as $3g \cdot 10$ tonnes vertically. This is also required by regulations [11].

The assumption that the logs acts as an evenly distributed load are made since the logs are normally tightened together with chains in order not to move during transport.

In general the truck drives empty every second run and therefore the loads on the timber bolster varies. When driving empty on an uneven road the bolster experience accelerations in all directions. Even though the trailer is empty the loads are significant due to the large accelerations. This was simulated by applying an acceleration of $10g$ in the x, y, z-directions. The demand on lowest natural frequency is used to avoid oscillating vertical beams when driving empty. The acceptance criterion is obtained from a reference calculation.

A load that is difficult to estimate is the abrasion from the sliding contact between the timber and the bolsters. This can occur both at loading and unloading but also when driving.

Impact loads occur when dropping a timber log on the bolster. Another possible impact load occurs when the logs are aligned by being hit against the bolsters. This is done when loading the timber to avoid misaligned logs. The lateral impact load is visualised in Figure 2.4 below.

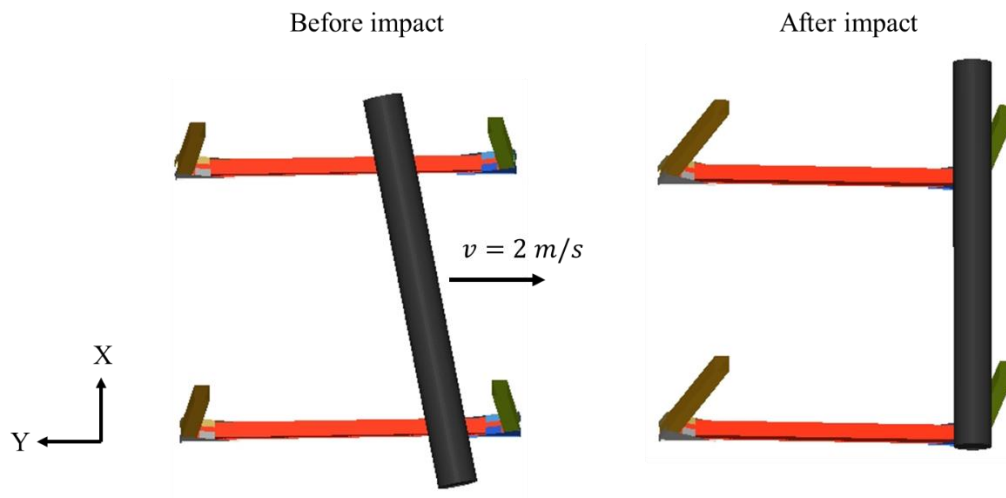


Figure 2.4: *Description of alignment of timber bolsters via an impact.*

The design guidelines for fibre layup are inspired by guidelines and recommendations from the aerospace industry [13, 14].

To avoid health concerns and negative environmental effects the material on Scania black and grey list should not be used.

3. Conceptual study

Fibre composites present unique opportunities for engineers in structural design. The ability to align the fibres thus tailoring the material and the component for the intended application offers significant potential in terms of weight saving.

During this thesis the initial concept phase was divided into separate areas in order to compare different characteristics. The overall idea was to discuss different characteristics while still keeping the relation between design features in mind. The process was divided into global geometry, cross section, manufacturing and material selection. By studying the global geometry the purpose was to determine how many parts the structure should consist of. A second section was devoted to a comparison of cross sections. Finally manufacturing and materials are discussed in the last two sections.

Throughout the process the authors discussed the concepts with engineers at Scania and Marstrom Composite AB who contributed with their deep knowledge within composite manufacturing.

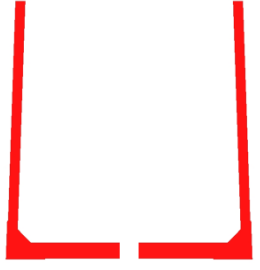
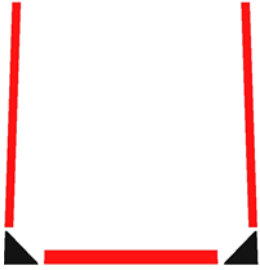


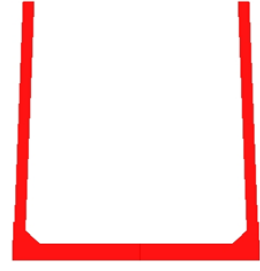
3.1 Global geometry concepts

The term global geometry is used to explain the overall geometry and design of the product with a clear focus on the number of parts and where to join them together. In Table 3.1 each concept is described and then a final comparison is made between the concepts in order to select the most appropriate global geometry, see Table 3.2.

In order to select a suitable global geometry several characteristics need to be taken into account for each concept. These are:

- **Continuous manufacturing possible:** The possibility to use continuous manufacturing methods is valued high since it increases the possibility to achieve low manufacturing cost. In general it also increases the capacity to mass-produce parts.
- **Joints in area of low stress:** Often the most critical part of a structure is the joints. This implies that its beneficial to position the joints in an area of low stress. This is therefore considered when analysing the global geometry.
- **Replacing parts:** If a structure fails its beneficial if it is easily replaced, especially within the transport industry where downtime is expensive. The ability to easily replace worn out or broken parts is therefore of interest.
- **Assembly complexity:** Especially when manufacturing a structure via several manufacturing methods the assembly is important to consider. The assembly complexity could increase manufacturing cost if the assembly time is too long.

Table 3.1: *Global geometry concepts and descriptions.*

Concept description	Visual representation
<p><i>Two parts</i></p> <p>A concept with two relatively big parts joined in the middle where the structure is less loaded. By producing the timber bolster in two parts the potential weight saving is high but challenges occur regarding the out of plane stresses in the corners. Automatization of manufacturing is also a challenging aspect.</p>	
<p><i>Separate corners and three beams</i></p> <p>A concept where the corners are produced separately makes it easier to produce using different methods and materials. The beams can for example easily be manufactured by a continuous process especially if the cross section is kept constant. A challenging aspect is the joints located close to the corners where the stresses are high.</p>	
<p><i>U-shaped bottom</i></p> <p>A U-shaped bottom will allow for continuous manufacturing of the vertical beams. Depending on the type of connection the vertical beams can be replaced if needed. The joints between the vertical beams and the bottom structure is challenging due to high stresses in that area.</p>	
<p><i>Corners and vertical beams in one part</i></p> <p>This concept has corners incorporated into the vertical beams. The horizontal beam can be manufactured via a continuous manufacturing process. Challenges with out of plane stresses in the corners remain.</p>	
<p><i>Monolithic structure</i></p> <p>If the whole structure is produced in a single piece no joints are needed but the out of plane stresses in the corners will challenge the designer. The potential weight saving is high but the manufacturing can become complicated, especially for large series.</p>	

The concepts were compared systematically by implementation of an evaluation matrix. Weight factors were used to account for the relative importance between the characteristics.

The concept achieving the highest sum of points was regarded as most suitable. The results are listed in Table 3.2 below.

Table 3.2: *Evaluation matrix for global geometry concepts.*

Global geometry concept	Continuous manufacturing possible	Joints in area of low stress	Replacing parts	Assembly complexity	Sum
<i>Weight factor</i>	10	7	6	5	
Two parts	2	8	2	8	128
Separate corners and three beams	6	2	10	4	<u>154</u>
U-shaped bottom	2	2	8	6	112
Corners and vertical beams in one part	2	2	8	6	112
Monolithic structure	1	10	1	10	136

Table 3.2 compares the different concepts. The concept of choice was the concept with separate corners and three beams. This concept allows flexibility in terms of manufacturing method, material and design.

3.2 Cross sections

Within this section the cross section of the beams are analysed. One of the critical loads for the structure is the bending of the vertical beams. For a beam subject to bending the cross section is of major importance and is therefore studied within this report. The evaluated characteristics for each cross section are:

- **Bending stiffness:** Bending stiffness is included in the comparison since several load cases includes loads implying bending of the vertical beams. The requirement on maximum displacement is easier to fulfill with a properly chosen cross section.
- **Impact robustness:** The robustness towards impacts was included to improve the structures resistance towards misuse and harsh conditions. The impact is most likely to occur when loading or unloading. For example an impact from a timber claw. A composite laminate is sensitive towards impacts on the free edges.
- **Ease of attachment:** The possibility to easily attach beams to the corners have an significant effect on the manufacturing and assembly. The possible weight saving can be decreased if the attachment concept is heavy or unreliable.
- **Twisting robustness:** Twisting of the vertical beams may occur when loading the truck and a log is moved in the x-direction. The log can then get stuck against a bolster and thereby causing a twisting motion on the bolster when moved in the x direction.

- **Aerodynamics:** The aerodynamic effects are considered small and has largest effect when driving empty. However a characteristic one should not forget is the possibility of sound generation from the bolsters. This effect can cause disturbing noise when driving empty but is difficult to predict and is given a low priority in this report.

These characteristics were then evaluated for each cross section and compared by using the same method as in Section 3.1 above. The comparison assumes a constant cross section along the length of the beams.

Table 3.3: *Evaluation matrix for cross sections.*

Cross section	Bending stiffness	Impact robustness	Ease of attachment	Twisting robustness	Aero-dynamics	Sum
<i>Weight factor</i>	10	7	6	3	1	
Solid rectangle	1	6	10	5	5	132
Rectangle hollow	8	8	10	6	2	<u>216</u>
Circle hollow	6	8	5	10	4	180
Ellipse hollow	8	6	3	7	5	166
I-beam	10	5	6	5	2	188
Hat-profile	9	5	8	5	3	191

As seen in Table 3.3 the most important characteristics were the bending stiffness and the robustness towards impact. Based on the evaluation above a rectangular cross section is superior. A rectangular cross section is robust and allows for several different manufacturing methods.

3.3 Manufacturing

A suitable manufacturing process is crucial to price and mechanical integrity and can often be the limiting factor for a successful design. Relevant manufacturing methods are discussed in the sections below. Further details can be found in Åström's book "Manufacturing of Polymer Composites" [15].

- **Autoclave:** By using autoclave and prepregs the mechanical properties becomes very good but it comes generally with a higher material cost. A prepreg carbon-epoxy structure generally requires 1-2 hours to cure in an autoclave. To increase the manufacturing speed one can cure several parts in the autoclave simultaneously. One of the reasons for the excellent mechanical properties is the curing under pressure that makes the composite more compact.
- **Vacuum infusion:** Vacuum infusion is a process that can be used when the fibre mats and matrix are bought separately. The process allows for cheaper moulds since the

temperature and pressure demands on the mould are low compared to for example autoclave and compression moulding. On the other hand it is difficult to manufacture large series efficiently.

- **Resin transfer moulding:** Resin transfer moulding (RTM) is a method where dry fibres are placed in a mould and impregnated with resin. This methodology is used within the car industry today and can produce large volumes at an acceptable cost. The degree of automatization can be high while still manufacturing complex geometries. The tools can be made cheaper compared to compression moulding since the mould does not have to resist high pressure.
- **Filament winding:** Filament winding is an efficient method in terms of high fibre content and a continuous manufacturing process. The properties of the matrix is crucial in order to not slow down production due to long curing times. A drawback is the requirements on a rotational symmetrical cross section in mass production.
- **Pultrusion:** Pultrusion is one of the most cost efficient methods when producing high volume products with constant cross sections. Similar to filament winding the curing of the matrix is crucial to maintain a continuous manufacturing process. Similar to filament winding one can achieve a high fibre volume fraction.
- **Compression moulding:** Compression moulding has a higher initial investment cost compared to RTM and vacuum infusion due to the need for a high quality tool that can resist temperature and pressure. However the possibilities to automate the process are present with advanced robotics and preregs.

Within this project pultrusion was chosen as manufacturing method for the three beams. This was mainly due to the continuous process and ability to keep the cost at a reasonable level. The corners have a more complex geometry and will be manufactured using RTM. The most relevant methods for the corners are RTM and compression moulding but due to the cheaper tool needed for RTM it was chosen as the preferred manufacturing method. The desired volume of 1000 units per year is almost small enough to motivate an autoclave manufacturing process, the autoclave has an advantage in terms of the possibility to vary cross section along beams, however this also leads to more complex tools.

3.4 Fibre materials

The main purpose of the fibres is to carry the loads, normally they have much higher strength and stiffness compared to the matrix.

- **Carbon fibre:** Carbon fibres are characterised by excellent mechanical properties but also a significantly higher price compared to glass fibres. However since carbon fibres are being more frequently used in large scale applications a reduction of the price is expected in the future [16, 17]. The problem with galvanic corrosion is an issue that arises especially around fasteners. This problem can be minimised by the use of stainless steel.

- **Glass fibre:** Glass fibres are significantly cheaper than carbon fibres but also has less good mechanical properties. Glass fibres have lower stiffness and are weaker but have a higher strain to failure when loaded in tension. By using glass fibre the risk of galvanic corrosion is avoided. A beneficial property of glass fibre is the good impact resistance [18].
- **Aramid fibre:** Aramid fibres are used for bulletproof vests and has a high impact resistance. Disadvantages are high price and low moisture resistance.

Based on a qualitative comparison both carbon and glass fibres were considered as feasible and were tried in more detailed calculations before deciding. It was concluded from these that glass fibres were unsuitable as structural fibre for this application due to their low stiffness as seen in Appendix B. Instead carbon was used as primary structural fibre whereas a surface layer of glass fibre is used to avoid galvanic corrosion. In summary the glass fibre is attractive due to good impact resistance whereas the carbon has excellent strength and a lower density, see Appendix B.

3.5 Matrix materials

In order to support the fibres and transfer loads between them the fibres are mixed with a matrix. Four matrices will be discussed namely polyester, vinylester, polyurethane and epoxy.

- **Epoxy:** Within the area of preregs epoxy is frequently used [13]. It is primarily used where high performance is prioritised over cost. As of today there are epoxy resin systems available for various manufacturing methods, for example RTM [19].
- **Polyurethane:** A thermoset matrix that has good abrasion properties is polyurethane however there are health concerns to consider when using polyurethane in production. The high fracture toughness makes it appropriate to use as a protective layer. Today there are polyurethane resins developed to be used within pultrusion manufacturing both for carbon and glass reinforcement [20]. Polyurethane can also be used in an RTM process [21].
- **Vinylester:** A widely used matrix is vinylester. It can be used for a wide range of applications and is generally cheaper than epoxy. When comparing to polyester the shrinkage while curing is lower for vinylester [15].
- **Polyester:** Polyester has similar properties to vinylester and is also frequently used, for example within the marine industry.

Due to the tough conditions for the timber bolsters the decision was taken to use polyurethane resin. Especially the good abrasion and impact resistance were valued as highly important. However no information detailed enough in order to conduct calculations was found regarding the properties of polyurethane composites with carbon or glass fibre and therefore the following calculations in this thesis were all based on epoxy to demonstrate the analysis methodology.

3.6 Conceptual design summary

A summary of the concept and its selected characteristics is listed in Table 3.4 below.

Table 3.4: *Summary of conceptual study.*

Characteristic	Chosen concept
Global geometry	4 corner pieces, 1 horizontal beam, 2 vertical beams
Cross section	Rectangular
Manufacturing method	Pultrusion (beams), RTM (corners)
Fibre	Carbon and glass (protective layer)
Matrix	Polyurethane

Based on the conceptual study a design was established according to Figure 3.1 below.

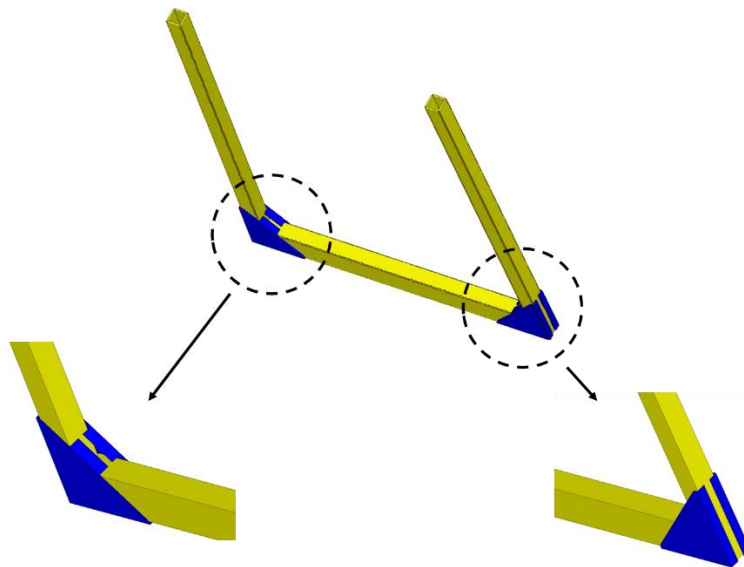


Figure 3.1: *Conceptual design of the timber bolster.*

As previously discussed the beams will have a constant rectangular cross section and the corners will be made as separate parts. More precisely each corner will consist of two parts. Each part will be designed according to Figure 3.2 including three flanges.

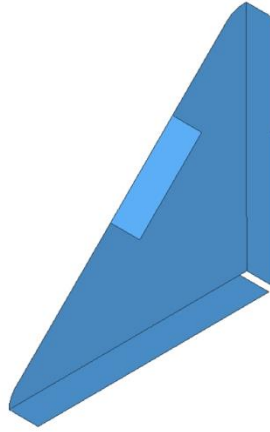


Figure 3.2: *Image of corner part in the concept.*

The vertical flanges primary serves to avoid peeling when loaded in the x-direction and the tilted flanges are used to increase the natural frequency and to avoid contact between timber and free edges of the laminates. On the bottom horizontal flanges are used to increase the bending stiffness as seen in Figure 3.3.

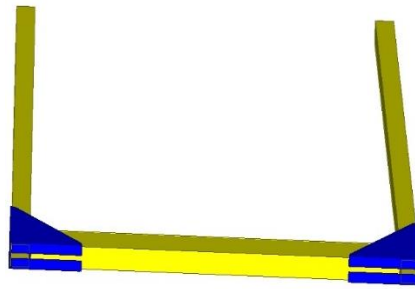


Figure 3.3: *Horizontal flanges are visualized on the bottom of the timber bolster.*

3.7 External feedback

After discussions with Marstrom Composite AB the possibility to use toughened epoxy was considered. The advantage of using a prepreg out of toughened epoxy and carbon is that one can produce high performance products and have more freedom when designing the geometry. A prepreg concept is also suitable for optimisation, see Section 6, and another advantage is that it requires a lower initial investment than e.g. pultrusion. Marstrom Composite AB also informed the authors that generally the pultrusion process uses a more brittle matrix. This is mainly due to the continuous manufacturing process that demands specific matrix characteristics. A study highlighting the properties of toughened epoxy is discussed in Appendix C where a rubber epoxy system is shown to significantly improve the fracture toughness and fatigue properties.

4. Business case for composite bolster

A fundamental aspect of designing a composite is the cost control. The cost reduction achieved by a lighter product leading to more payload has been compared with the increased cost associated with a fibre composite component. A comparison was made between an aluminium timber bolster and a composite bolster. The data that have been used for comparison is presented in Table 4.1.

Table 4.1: Data used for economic comparison of aluminium and composite bolster. The data for payload and an empty truck assumes aluminium bolsters.

Property	Used data	Reference
Price of aluminium bolster [kr]	20 000	[22]
Weight of loaded truck [kg]	64 000	-
Empty truck [kg]	18 000	-
Payload [kg]	46 000	-
Income for transporting timber[kr/m ³]	44	[23]
Density timber [kg/m ³]	400	[24]
Fuel consumption [l/ (tonnes · km)]	0.02	[2]
Transport distance [km]	100	[3]
Number of transports per year	1200 (50% empty)	-
Fuel price [kr/l]	12	-
Number of bolsters per truck	8	-
Time until breakeven for composite bolster [years]	5	-

The comparison includes an increased income due to an increased payload and a decrease in cost due to lower fuel consumption when driving empty. Table 4.2 below presents a pure comparison between an aluminium and a composite timber bolster.

Table 4.2: Increased income and decreased cost due to lower weight of composite bolster, compared to aluminium.

Weight saving per bolster [kg]	Increased payload [kg]	Increased income from increased payload [kr/100km]	Decrease in fuel cost due to lowered weight [kr/100km]	Economic gain after 5 years [kr]
1	8	0.88	0.192	3216
2	16	1.76	0.384	6432
3	24	2.64	0.576	9648
...
70	560	61.6	13.44	225 120

However the economic gain from a lighter bolster should cover the increased cost for a more expensive bolster. This needs to be accounted for and was calculated and can be seen in column three in Table 4.3 below. Furthermore Table 4.3 also includes a weight saving demand on the bolster due to the increased price of a lighter bolster in order to have profitability within five years.

Table 4.3: Table of weight saving demand on a composite bolster due to higher initial cost.

Price per bolster [kr]	Total cost for 8 bolsters [kr]	Increased cost compared to aluminium bolsters [kr]	Weight saving demand per bolster [kg]
20 000	160 000	0	0
21 000	168 000	8000	3
22 000	176 000	16 000	5
...
35 000	280 000	120 000	38

The demand on weight saving in column four of Table 4.3 is calculated by comparing the economic gain from Table 4.2 and the increased cost from the third column in Table 4.3. This comparison gives a breakeven point that can then be visualised in a graph for different amount of weight savings. The conclusion is that saving 1 kg is worth 80 kr/year. Figure 4.1 displays the trade-off between the price and lowered mass. The dashed line shows the customers willingness to pay in order to break even within five years.

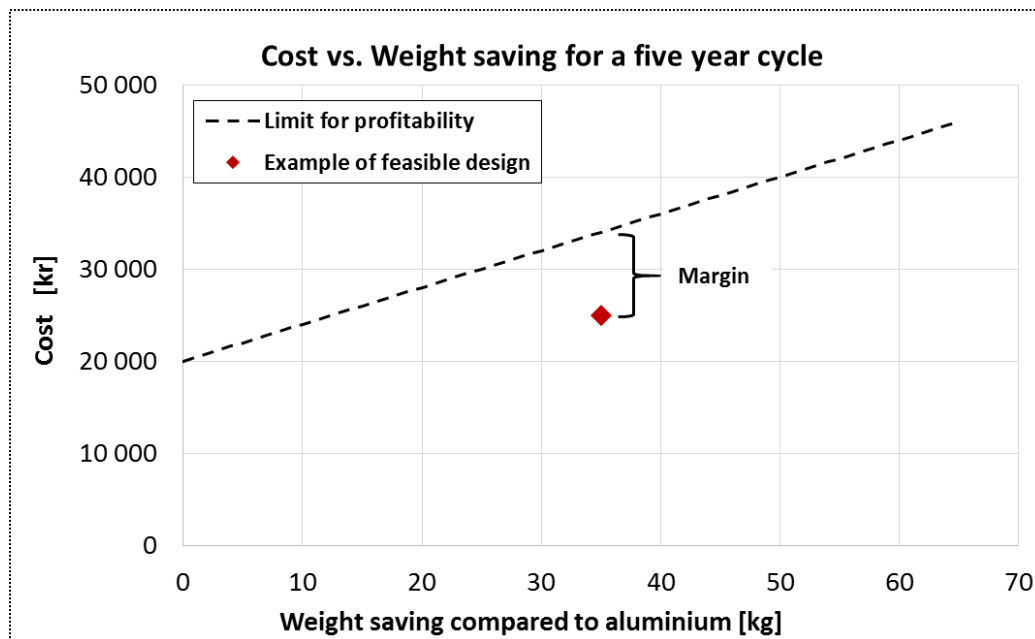


Figure 4.1: Graph displaying the relationship between the price and required weight saving compared to aluminium for one bolster.

As an example a red point is indicating a feasible composite design. The vertical distance from the square to the dashed line is the margin between the manufacturing cost and the customers willingness to pay. The cost only includes manufacturing and does not include,

overhead costs, marketing or other costs. Based on the assumptions the increased income from increased payload represents 80% of the margin compared to aluminum and the remaining 20 % of the margin is due to lowered fuel costs. The total manufacturing costs were estimated based on the raw material cost and a relation between the raw material cost and total manufacturing cost. As seen in Table 4.4 the relation varies depending on manufacturing process.

Table 4.4: *Relationships between process and material costs in percentage of total manufacturing cost.*

	Material cost [%]	Manufacturing process [%]
Autoclave	50	50
Other methods e.g. pultrusion	30	70

For determining the raw material cost discussions with the materials department at Scania and Marstrom Composite AB took place. A price of 13.5 eur/kg was used for the structural carbon fibre and 2 eur/kg for the protective glass fibre. The matrix price was assumed to be 5 eur/kg. By using these numbers the manufacturing cost for e.g. pultruded products could be found. In order to compensate for the higher material price related to prepregs for the autoclave manufacturing an additional 4 eur/kg were added to the material cost. Note that the relations displayed above are simplifications and varies depending on manufacturing volumes. For example an expensive machine might be a high initial cost that one later can benefit from.

5. Modelling methodology

Modelling composites using finite element method is a process that can be performed in different ways depending on used modelling tools and solver compatibility. The method used in this thesis used Hypermesh as modelling tool and is outlined below in Figure 5.1. The modelling is based on classical lamination theory [25].



Figure 5.1: *Simulation driven design workflow.*

5.1 Prepare CAD model

The general workflow began with a CAD drawing of the structure created in CATIA V5. Once the geometry is imported into Hypermesh it was necessary to conduct extensive work to prepare the geometry for FE-analysis.

5.2 Generate mesh

Once a basic model was created a mesh needed to be generated. Whether it is necessary to use 2D elements to save computational time or 3D elements to get a better overall representation becomes a highly relevant question for these types of structures. Composite structures tend to be relatively thin making them suitable for modelling using 2D shell elements. 3D elements are more suitable for composite analysis when a detailed analysis of particular areas where a three dimensional stress field might be relevant to consider such as bolted joints.

In this thesis a 2D shell mesh was used for the main structure and the optimisation procedure. For the more isolated bolted joint and failure criteria analysis a 3D mesh was used in the proximity of the bolted joints (section 7.4).

5.3 Create laminate

The main difference between modelling isotropic structures and composites is that the later consists of several plies with anisotropic characteristics that are to be coupled to the elements. The methodology in Hypermesh is that composite properties are applied to shell elements. This is done with the *create ply* function which allows creating plies with a selected material, thickness and fibre orientation and allowing each ply to be assigned to a selected set of elements. After the plies have been created they are to be stacked in order to form a laminate. This is done with the *create laminate* option which provides a visual representation of the stacking sequence and allows the use of practical functions such as symmetry in laminates. The stacking sequence follows the element normal thus making it important to check the normal direction of the elements in the model. As seen in Figure 5.2 the shells are changed from conventional shell elements with corresponding properties to composite shells.

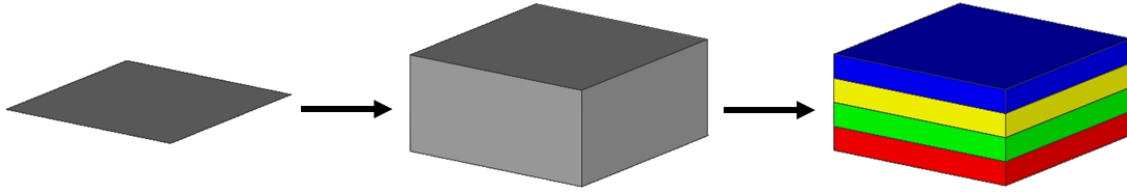


Figure 5.2: *Composite shell structure in Hypermesh. The same element is displayed with different view settings (traditional shell, shell with thickness representation and composite).*

Each composite ply contributes with its own thickness and mechanical properties in various directions to form the properties of the element. In Figure 5.2 the shell consists of four plies, but an actual model can consist of any number of plies stacked into the same shell element.

5.4 Composite alignment

Composites are anisotropic materials which makes the orientation of the fibres critical in the design. As mentioned above the created composite plies have a specific orientation which is used to represent the fibre direction. However, these ply orientations are only relative to each other, see Figure 5.3. It is therefore needed to align the plies of the laminate against a reference. In Hypermesh this is done by assigning an orientation directly to the elements and thus creating an axis that the plies are to be oriented relative to.

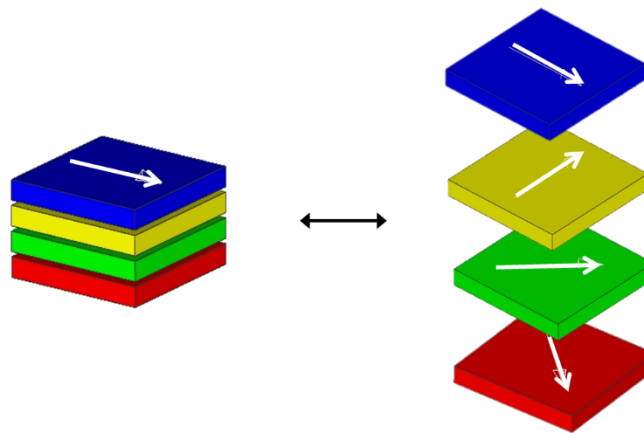


Figure 5.3: *Fibre orientations in a shell element. Blue, yellow, red and green represents 0° , 90° , 45° and -45° orientations respectively.*

The benefit of this method is that one can create a laminate consisting of e.g. 25 plies at one occasion and aligning all of them with respect to the geometry of the component with one operation. Also since each element can be oriented independently it becomes simpler for the user to align the laminate onto a more complex geometry.

6. Optimisation of fibre composite timber bolster

This section will describe and utilise a method where both material and geometry are changed simultaneously to achieve a lighter product. The possibility to change material and geometry holds for both anisotropic and isotropic materials. However a major difference is that for anisotropic materials one can also optimise the material orientation. This was utilised when optimising and designing a fibre composite structure within this thesis. The optimisation was made using Hypermesh as pre-processor and Optistruct as solver. These design tools use a ply based modelling approach as presented in Section 5.

6.1 Optimisation methodology

Prior to starting the optimisation the design space was defined. Within this thesis the design space was limited to the two vertical beams as illustrated in Figure 6.1.

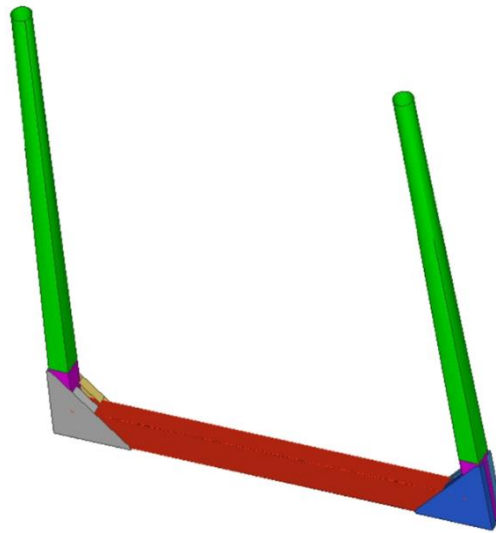


Figure 6.1: *Timber bolster with design space visualised in green.*

Due to the joints in the corners the design space was limited to the part of the vertical bolsters not in contact with the corners. A second restriction was applied to the design space, namely that a protective layer of glass fibre has to be placed on the outer surfaces of the bolster. The optimisation was thereby limited to the carbon fibre layers within the vertical beams. The overall procedure for the optimisation was performed in three steps. These are described graphically in Figure 6.2 together with the verifying step used to validate the design against the structural demands from Section 2.2.

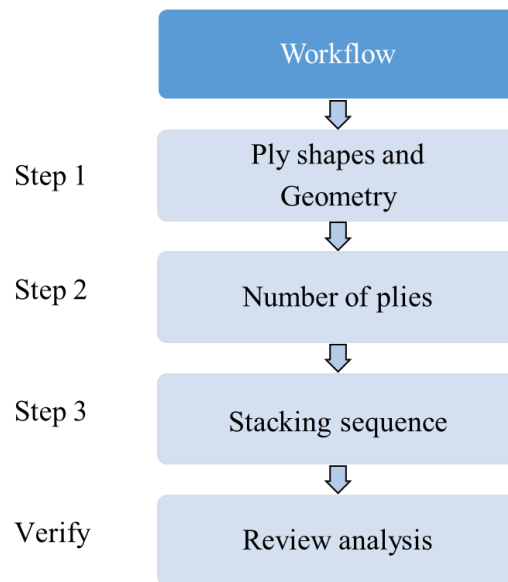


Figure 6.2: *General optimisation workflow.*

6.1.1 Step1. Geometry and ply shape optimisation

The first step served to find the optimal combination of the cross sectional geometry and the ply shapes. By keeping the rectangular cross section at the bottom of the design space constant and varying the cross section at the top, the geometrical shape varied linearly from the bottom to the top. The cross section at the top was used as design variable and was allowed to vary according to the cross sections described in Figure 6.3 below, where the area in contact with the timber is marked in yellow.

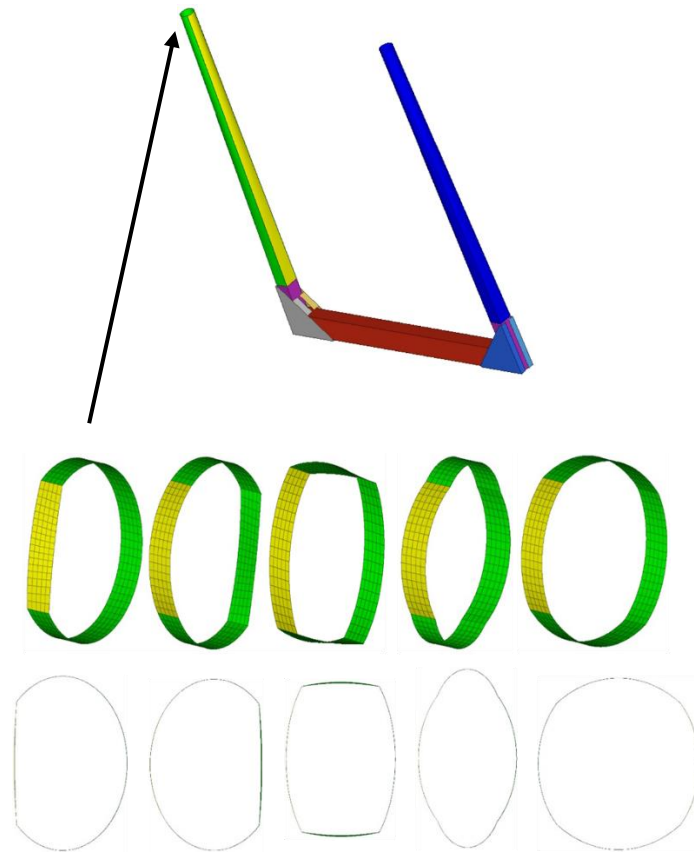


Figure 6.3: *Visualisation of shapes used and their application at the top of the bolster.*

Note that the cross sectional shapes could also be combined and varied simultaneously. An illustrating example is when combining the first two cross sections from Figure 6.3 in order to obtain a new shape as seen in Figure 6.4 below.

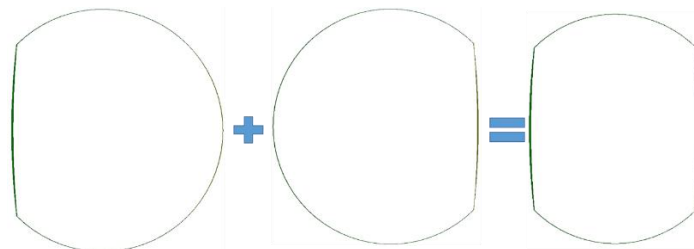


Figure 6.4: *Visual explanation of how shapes can be combined to achieve various cross sections.*

When designing the allowable geometrical shapes the contact area between the timber and the bolster, marked yellow in Figure 6.3, was not allowed to be too small. A too small contact area would lead to problems with abrasion and a less robust design.

The composite optimisation was performed in order to find the ply shapes and thickness distributions for each fibre direction that gives the lightest design. In other words the thickness distribution determines both how much material is needed in total and how much of it that should be oriented in each fibre direction. For reasons regarding manufacturing four fibre directions were used within this project namely 0° , 90° , 45° and -45° . For each one of

the four fibre directions an optimal and unique thickness distribution was found as illustrated for the 0° and 90° orientations in Figure 6.5.

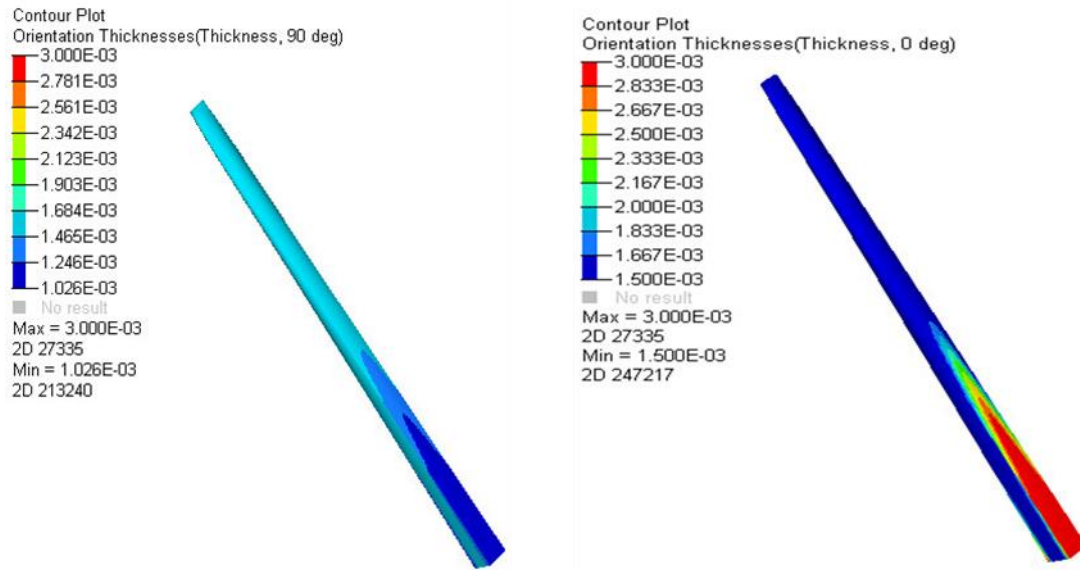


Figure 6.5: Thickness distribution of 90° (left) and 0° plies (right).

The thickness was achieved by optimisation with continuous design variables. Each fibre direction has its own continuous design variable for each element. This is to capture the individual thickness distribution for each fibre direction. For example a mesh with 10 elements leads to 4·10 design variables.

For a manufacturing method based on plies, the ply shapes and thickness distributions according to Figure 6.5 is difficult to achieve due to the varying thickness and complex ply shape. The remedy is to divide the generated ply shape in Figure 6.5 into four thinner ply shapes that together form the original shape, as presented in Figure 6.6.

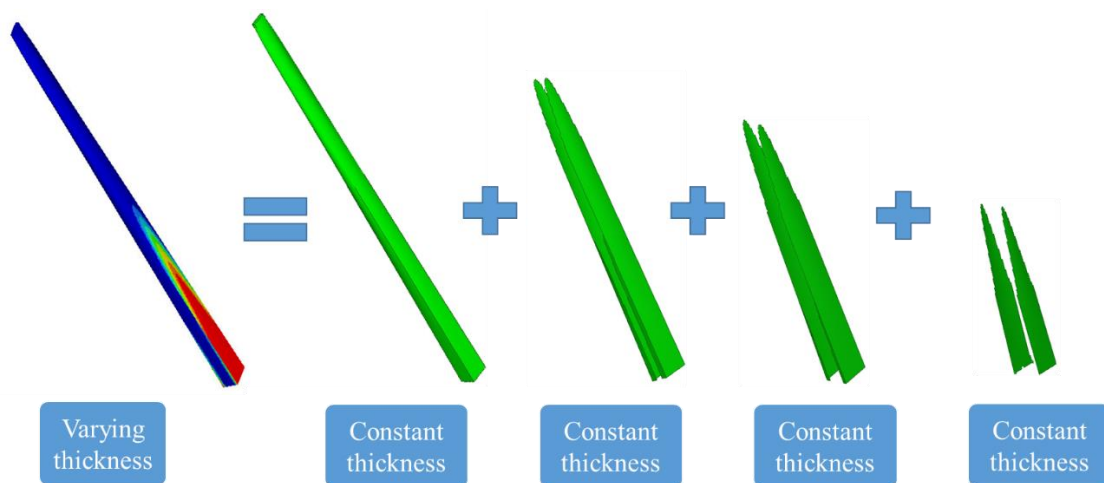


Figure 6.6: The varying thickness of the 0° fibre orientation divided into four plies with constant thicknesses.

In total this generated 16 ply shapes, four ply shapes per fibre orientation. Before moving into Step 2 of the optimisation a manual operation was performed to adapt the design to be more realistic in terms of manufacturing. More precisely the shapes displayed in Figure 6.6 were simplified into more realistic ply shapes. An example of this can be seen in Figure 6.7 below where a complex shape is simplified to better agree with a realistic manufacturing process where mats are to be cut and placed.

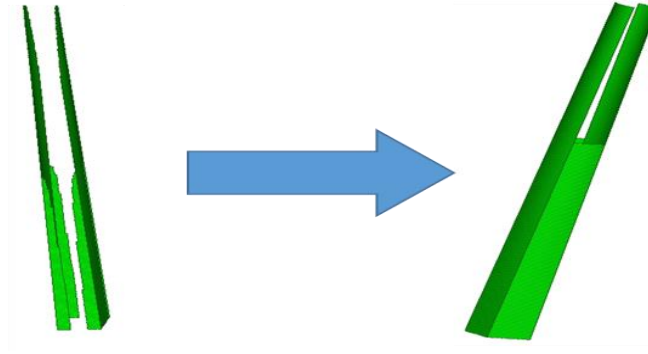


Figure 6.7: *Simplification of generated ply shapes.*

The procedure of simplifying the ply shapes was carried out on all of the 16 plies and were together with the geometrical shape the results from Step 1. A summary of Step 1 can be seen in Figure 6.8 below.

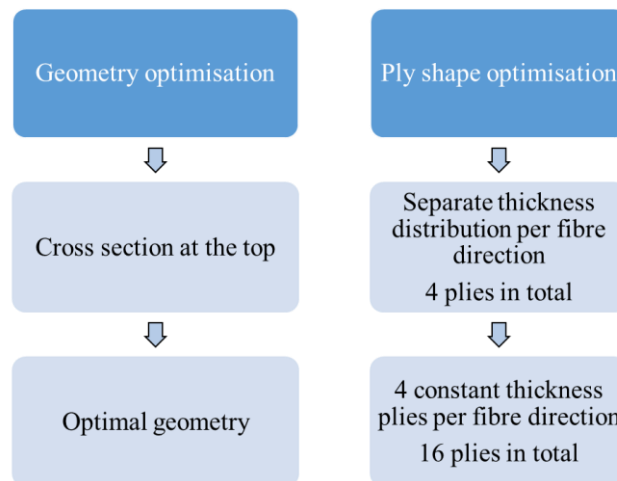


Figure 6.8: *Procedure for Step 1 showing the combined geometry and composite optimisation.*

The geometry found in Step 1 was kept constant for the remaining steps. Step 2 and 3 deals solely with composite layup optimisation.

6.1.2 Step 2. Optimal number of plies

In Step 2 the amount of plies needed for each ply shape was to be determined. The plies used for manufacturing have a constant predetermined thickness. This implies that the 16 plies

from Step 1 only can be multiples of that ply thickness. For example if one knows that the manufacturing will be done with 0.25 mm thick plies the thickness can only be multiples of 0.25 mm, i.e. 0, 0.25 and 0.5 mm. Thereby this step results in a discrete number of plies needed for each fibre direction. In summary Step 2 of the optimisation results in a discrete number of plies for each ply shape as depicted in Figure 6.9. Note that the figure illustrates the procedure using four of the 16 ply shapes. The actual optimisation was made using all 16 ply shapes simultaneously.

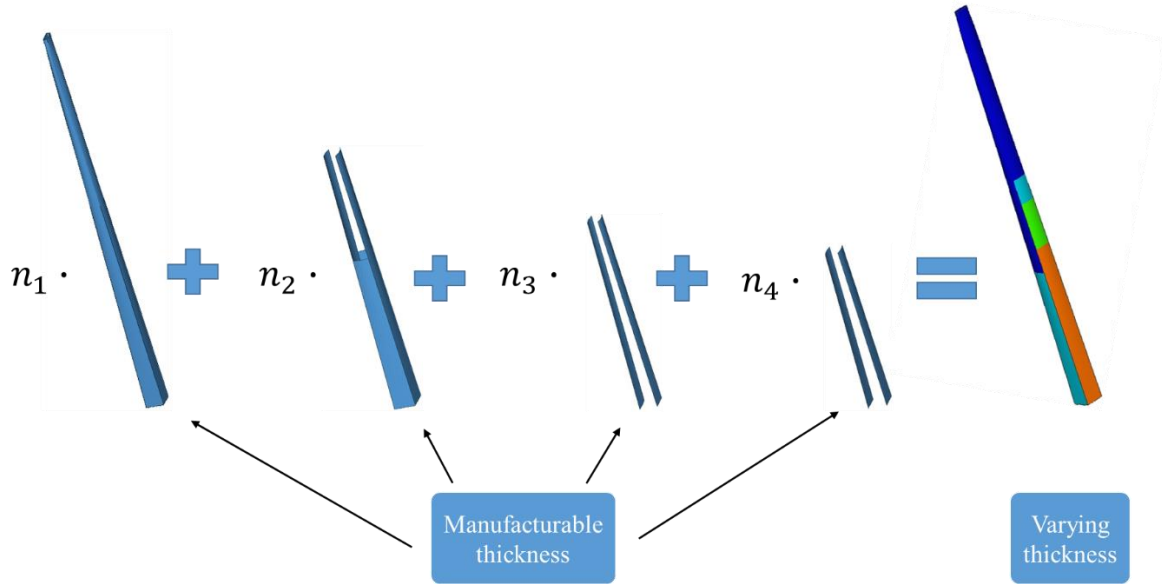


Figure 6.9: Manufacturable ply shapes that together form the design. The variables $n_{1,2,3,4}$ denote the needed number of plies of each shape.

6.1.3 Step 3. Stacking sequence optimisation

The third step aims to find the optimal stacking sequence of the plies retrieved from Step 2. This is a pure shuffling operation that do not affect the weight of the structure. Regarding the modelling technique the third step differs from the previous steps by taking into account the effect of the stacking sequence. In contrast the first two steps were performed using the simplified approach of smeared laminates. This was done in order to eliminate the stacking sequence effects. In summary the third step is a pure shuffling optimisation where no material is added or changed. This step finds the optimal stacking sequence and thereby finalises the optimisation.

6.1.4 Verification

The methodology is not complete without a verifying analysis on the optimised design. A final comparison against the structural demands in Section 2.2 was made and if needed adjustments could be done to finalise the design. An example could be to modify the layout of the adjacent non-design space in order to be more consistent with the optimised design.

6.2 Analysis setup

This section describes the setup used when applying the methodology described in Section 6.1 above. The first step in the optimisation was set up according to

$$\text{Step 1} \begin{cases} \text{min mass} \\ \text{s.t } u < 35 \text{ cm} \\ f_1 > 7 \text{ Hz} \end{cases} \quad (6.1)$$

where u is the maximum displacement and f_1 is the lowest natural frequency and the used manufacturing constraints are listed in Table 6.1 below.

Table 6.1: *Applied manufacturing constraints at Step 1 of the optimisation.*

Constraint formulation	Constraint explanation
Balance $\pm 45^\circ$	Equal number of 45° and -45° plies
$6 \text{ mm} < t < 13 \text{ mm}$	Total laminate thickness
$5 \% < \text{Plypct} < 70 \%$	Percentage of a single fibre orientation
Plydrop = 5 %	Ply drop-off in laminate

The manufacturing constraints are based on laminate design guidelines in Section 2.2. For example the drop-off constraint is commonly used to avoid stress concentrations and the constraint on equal number of $\pm 45^\circ$ oriented plies is used to avoid unbalanced laminates. The thickness and shape of the plies together with the geometry shapes defines the design variables. The allowable geometry was defined by allowing the cross section at the top of the bolster to vary according to Figure 6.3. Furthermore these 16 plies were then together with the geometry the foundation of the second step of the optimisation.

The second step of the optimisation was set up according to

$$\text{Step 2} \begin{cases} \text{min mass} \\ \text{s.t } u < 35 \text{ cm} \\ f_1 > 7 \text{ Hz} \\ \text{FI}_{\text{strain}} < 0.36 \\ \text{FI}_{\text{strain}} < 1^* \end{cases} \quad (6.2)$$

where * indicates failure criterion for max load in contrast to the constraint for the fatigue load cases. The manufacturing constraints applied during Step 2 are listed in Table 6.2.

Table 6.2: *Manufacturing constraints applied during Step 2.*

Constraint formulation	Constraint explanation
Balance $\pm 45^\circ$	Equal number of 45° and -45° plies
$6 \text{ mm} < t < 20 \text{ mm}$	Total laminate thickness
$5 \% < \text{Plypct} < 70 \%$	Percentage of a single fibre orientation
Plydrop = 5 %	Ply drop-off in laminate
Plythk = 0.25 mm	Manufacturable thickness of plies, constant thickness

The manufacturable ply thickness of 0.25 mm was added to achieve a more realistic design. The maximum strain constraint was applied to the carbon layers to ensure resistance towards failure.

The final step performed was a shuffling optimisation which was set up according to

$$\text{Step 3} \begin{cases} \text{min compliance} \\ \text{s.t } u < 35 \text{ cm} \\ f_1 > 7\text{Hz} \end{cases} \quad (6.3)$$

where the goal was to find the optimal stacking sequence. The maximum number of consecutive plies with the same fibre angle was constrained to three and the $\pm 45^\circ$ plies were forced to be stacked as pairs.

The design was then verified against the structural demands. Based on the final layup of the design space the layup of the non-design space was adjusted to smoothen the transition between these areas, seen as the transition between purple and green in Figure 6.1. Moreover the thickness of the protective glass fibre layer was increased for the whole structure and then the structure was validated against failure via both the Tsai-Hill criterion and the maximum strain criterion. To further verify the structure an analysis was made without the protecting layer of glass fibre, this was done to verify that even if the protective layer is damaged the structure can still withstand the loads.

6.3 Results

The results are presented with focus on the final design. Regarding Step 3 no significant effect was obtained and therefore the stacking sequence was determined manually using the guidelines. The final layup of the vertical beams can be seen in Table 6.3. Due to symmetry only half of the layup is visualised.

Table 6.3: *Laminate stacking sequence of optimised vertical beams.*

Material	Thickness [mm]	Fibre orientation [°]
Glass	0.5	45
Glass	0.5	-45
Carbon	0.25	0
Carbon	0.25	0
Carbon	0.25	0
Carbon	0.25	45
Carbon	0.25	-45
Carbon	0.25	0
Carbon	0.25	0
Carbon	0.25	90
Carbon	0.25	0
Carbon	0.25	0
Carbon	0.25	0
Carbon	0.25	45
Carbon	0.25	-45
Carbon	0.25	0
Carbon	0.25	0
Carbon	0.25	90
Carbon	0.25	0
Carbon	0.25	0
Carbon	0.25	0
Carbon	0.25	45
Carbon	0.25	-45
Carbon	0.25	0

As previously mentioned a final adjustment was made to smoothen the transition from the non-design space to the design space. In order to have a constant layup for the non-design space the layup was modified from a pure quasi-isotropic layup to a layup with slightly higher 0° fibre orientation content, see Appendix D. The final thickness distribution of the timber bolster is displayed in Figure 6.10 below.

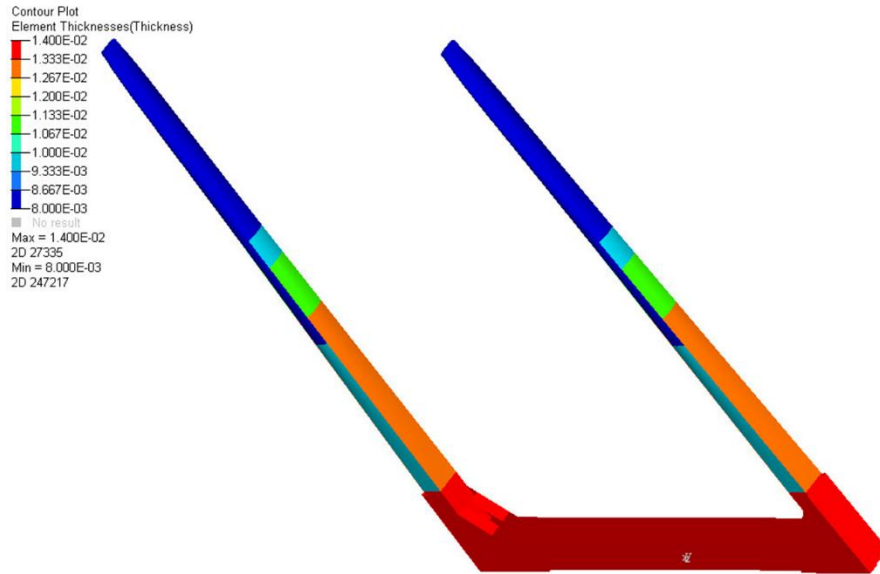


Figure 6.10: *Thickness distribution of optimised design.*

The displacement when loading with the maximum bending load of $0.5g \cdot 10$ tonnes is displayed in Figure 6.11 below.

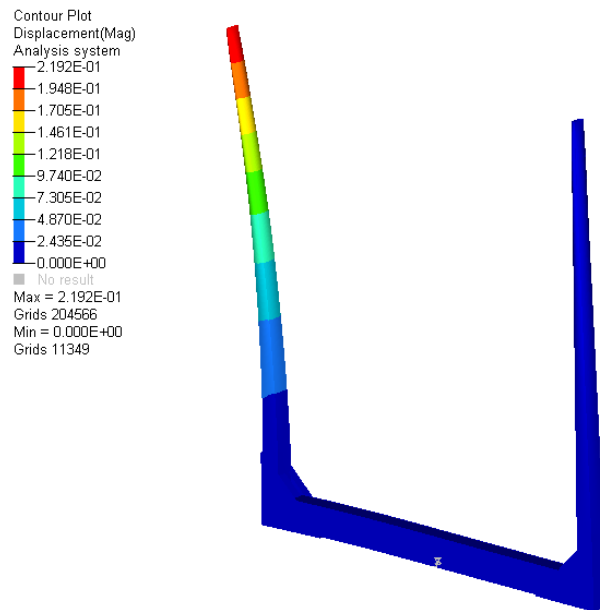


Figure 6.11: *Displacement when subjected to maximum bending load.*

A final comparison was then made between the optimised composite structure, the non-optimised composite structure from the conceptual study and the aluminium structure used as reference. The non-optimised structure had a zero dominated layup similar to the optimised but with the difference that there are no cut ply shapes and vertical beams that are made with constant rectangular cross sections. All plies are equal in size and cover the whole structure. The results are presented in Table 6.4.

Table 6.4: Comparison between timber bolster designs. Carbon stands for carbon epoxy and glass stands for glass epoxy used in the protective outer layers.

	Optimised composite	Non-optimised composite	Aluminium
Total mass [kg]	87 (carbon 70, glass 17)	108 (carbon 89, glass 19)	136
Mass non-design space [kg]	48	-	-
Fulfils list of requirements	Yes	Yes	-
Max displacement [cm]	22	19	-
Manufacturing method	Autoclave	Pultrusion (beams), RTM (corners)	-
Series length	<1000	>1000	>1000
Estimated price [kr]	31 600	28 200	20 000

The material data used for the composite designs are found in Appendix B. In total the geometry optimisation lowered the weight by 10 kg compared to the non-optimised design. The remaining 10 kg of mass reduction was achieved by the composite layup optimisation. By inserting the results into the graph in Figure 4.1 the graph in Figure 6.12 was obtained. The conclusion is that the optimised design provides a profitable business case.

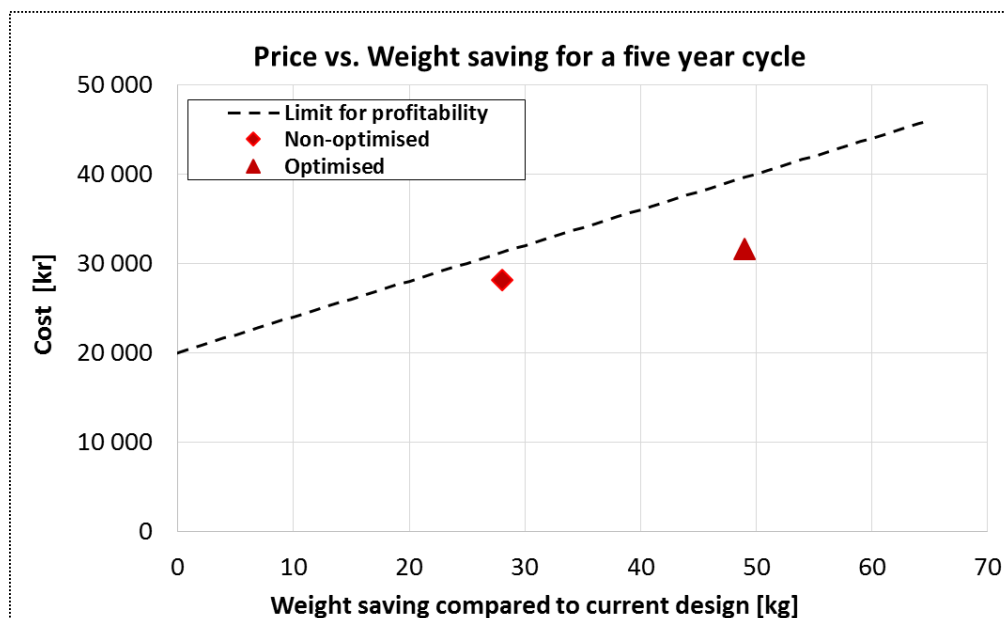


Figure 6.12: Economic comparison between composite concepts and the aluminium reference.

6.4 Discussion of optimisation procedure

As seen in Figure 6.12 the potential business case for using composite timber bolsters is relevant for further investigation. The optimised concept indicates a higher margin but also includes a more complex manufacturing due to the more complex geometry and ply shapes. To get the full picture one should remember that the numbers displayed in Figure 6.12 are for one bolster. It is possible to have 8 or more bolsters on one truck and thereby the potential weight saving for the whole vehicle is even bigger.

Within this thesis the mass was reduced mainly by using three approaches, changing material, geometry and material orientation. The results from the optimisation procedure shows that neither the geometry or the layup should be neglected when trying to lower the mass.

The resulting ply shapes are visualised in Appendix E. The optimised ply shapes show that only the 0° plies have complex shapes that needs extra processing during manufacturing. The fact that the 90° , 45° and -45° plies do not need any extra cutting will keep the production cost down.

The shuffling optimisation in Step 3 gave no significant contribution to the results in this case. The objective to lower the compliance was not possible and therefore the shuffling optimisation was not considered. Instead the stacking sequence was manually decided.

The modification of the non-design space was done to decrease the difference in layup between the non-design space and the design space, especially in the transition from the green to the purple area as seen in Figure 6.1. Going from one layup to another within the same component is an area of future work were there are opportunities for improvements. This is closely related to the manufacturing aspects as one might consider issues related to where to place the cuts or how to position the plies

The most critical layer was the 90° layer, mainly due to the low allowable strain limit in the direction transverse to the fibres. One might expect that the most critical would be compression of the composite but as mentioned the most critical load was the tension of the 90° layer. The distribution of the maximum strain criterion for the structural carbon fibre layers can be seen in Appendix F.

In Table 6.4 the recommended manufacturing method is autoclave but other methods such as RTM are also relevant. The methods stated in Table 6.4 should be seen as suggestions and not definite answers. For example an autoclave process can vary significantly in terms of automatization which makes it suitable for different manufacturing volumes.

As expected the time for setting up and performing an optimisation is significant even though a state of the art software was used that supported the three staged optimisation procedure. In the end, the business case depends on the costs associated with the product and the value it creates for the customer.

The skills developed and needed to fully take advantage of the optimisation procedure includes FE-modelling, economics and manufacturing. The modelling skills are self-explanatory but one should not forget the manufacturing aspects. An engineer experienced in manufacturing has the knowledge of how to compare manufacturing costs with the potential weight saving.

Within this thesis the optimisation was limited to the vertical bolsters even if the whole structure was analysed and forced to meet the demands for the final design. The reason for this simplification is described above and leads to a less optimal design. However the significant weight reduction indicates that there is a possibility to reduce the weight by using optimisation. On a more detailed level the minimum laminate thickness also plays a significant role for the overall weight of the component. The minimum thickness was set to 8 mm including 2 mm of glass fibres to increase the margin to protect from abrasion and impact during loading as well as acting as a protective layer against corrosion.

A possible improvement would be to analyse the need of a protective glass fibre layer in more detail, especially since the mass contribution from glass is significant. The rubber-epoxy based matrix in Appendix C might be an alternative but further investigations are needed. One should also remember the protection against corrosion provided by the glass fibre layers.

In general the displayed methodology combining composite and geometry optimisation shows significant weight saving potential. By the use of Optistruct one can combine several types of optimisation to achieve a lighter design. Via small adjustments the potential weight saving by varying fibre angles more freely could also be investigated. Within this thesis this was not done but it's an area of future work. However the used methodology based on standardised fibre orientations has several advantages in manufacturing.

6.5 Conclusions of optimisation

The following conclusions were made from the optimisation procedure:

- The potential weight saving compared to an aluminium design is high when using optimisation driven design of fibre composites.
- Both geometry and composite layup have a significant impact on the weight saving.
- Significant weight saving is possible if the protective glass fibre layers can be minimised.

7. Joints in composite structures

Among the most important parts of the design of components in structural applications in general and for composites in particular are the joints. The occurrences of various types of joints in structures are most often a necessity. It can be very difficult, and sometimes either impossible or result in a more expensive outcome, to design a monolithically shaped structure that fulfils all of the requirements of a finished product. It is therefore important to consider joints in the design of composite structures. This section aims to describe benefits and drawbacks of joining types, failure modes, guidelines and analysis in composite joints. It also contains a methodology for a detailed FE-analysis of bolted joints.

7.1 Joining techniques

The most common methods of joining composite laminates are adhesive bonding and mechanical fastening. Both of these have various advantages and disadvantages compared to each other. Some are general whilst others are more specific to each application. A qualitative comparison of the two types of joints is listed in Table 7.1.

Table 7.1: Comparison of mechanical and adhesive joints [15, 26, 27]. A plus sign indicates an advantage and a minus sign indicates a disadvantage.

Property	Mechanical joints	Adhesive joints
Low stress concentrations	-	+
Damage from hole generation	-	+
Weight	-	+
Fatigue life	-	+
Damage tolerance	-	+
Potential for creep	+	-
Fretting problems	-	+
Peel strength	+	-
Galvanic corrosion	-	+
Environmental sensitivity	+	-
Joining dissimilar materials	+	-
Sensitivity to differences in thermal expansion	+	-
Component shape and surface control	+	-
Possibility of disassembly	+	-
Possibility for inspection	+	-
Thickness limitations	+	-
Smooth external joint surface	-	+
Cost	-	+

As seen in Table 7.1 adhesively bonded joints offer advantages in terms of fatigue performance and are a more efficient method because it offers more potential to reduce stress concentrations [13]. They have potential to reduce galvanic corrosion and are a lightweight and relatively low cost option. However, adhesively bonded joints are highly dependent on surface quality, manufacturing deficiencies (such as poor fitting) and environmental exposure [13, 26]. They are also primarily intended for bonding thin components rather than thick ones. Bond quality has been a continuous problem and even though X-ray techniques have been

used there is currently no method to guarantee the load transfer capability of a bonded joint [13]. For these reasons mechanically fastened joints tend to be preferred in structurally critical areas.

Mechanically fastened joints e.g. bolted joints have the advantage that they are relatively insensitive to environmental exposure and also to various properties of the components that are to be joined such as surface quality and differences in coefficient of thermal expansion, CTE [27]. Although the tooling costs are low, drilling holes in composite laminates is a task requiring great care to avoid damaging the composite in terms of crack initiation and fibre misalignment. Another important aspect is that composites tend to creep with time when subjected to compressive loads resulting in a loss in pretension force. This means that designing of composite bolted joints differs fairly from metal joints.

The vehicle industry in general and the automotive industry in particular have very high demands on adaptability to a modular system and ability for disassembly of their components. Due to these reasons this project is intended to evaluate bolted joints in composite structures.

7.2 Failure modes in bolted laminates

Failure in composites can be a complicated phenomenon and is an area that is currently undergoing intense research. The anisotropic behaviour, tensile and compressive differences as well as the very low out of plane capabilities of composites all contribute to the fact that two composite plates that might look similar for the naked eye might behave and fail in very different ways. Drilling a hole and adding a bolt adds another aspect to be considered into an already complex area of engineering analysis. This section provides a brief description of the more common failure modes in bolted composite joints as depicted in Figure 7.1 below.

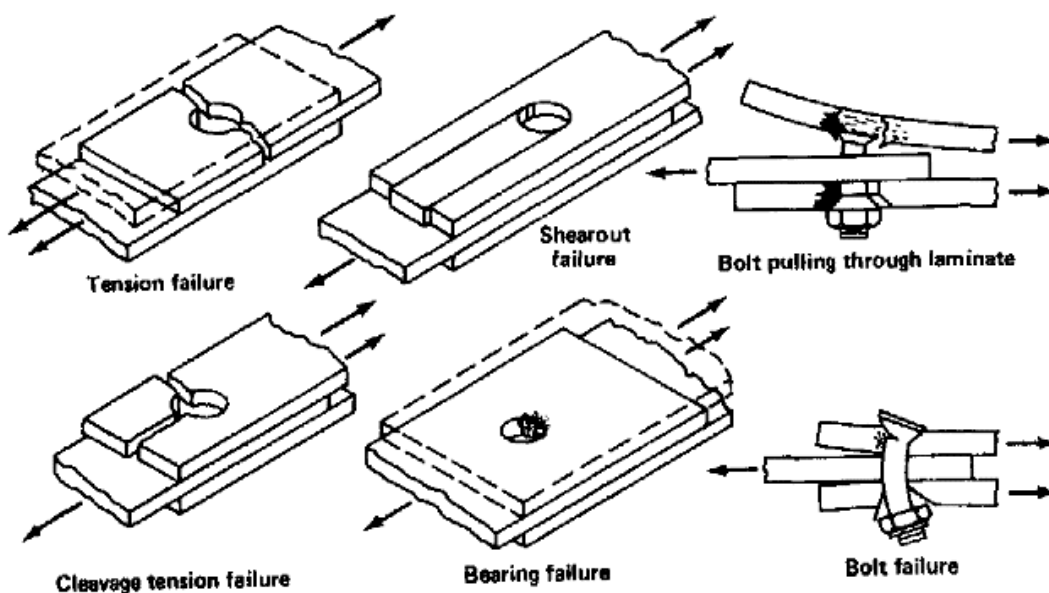


Figure 7.1: Common failure modes of bolted composite joints [13].

- **Tension failure:** Tension failure, also known as net-section failure, is when a laminate separates across the line of the bolt, as seen in Figure 7.1 above. It is an abrupt failure mode which tends to occur when there is an insufficient width of the laminate, see Figure 7.2, as well as when the laminate consists of too few plies oriented in the loading direction [27, 28].
- **Bearing failure:** This is a ductile and primarily compressive failure mode occurring close to the contact region at the edge of the hole. The compressive loading from the fastener head onto the hole edge leads to buckling and fibre kinking as well as matrix crushing [28, 29].
- **Cleavage tension failure:** This is an abrupt failure mode which tends to occur when the distance from the laminate edge to the hole is too small as well as when there is an insufficient amount of cross-ply i.e. plies oriented $\pm 45^\circ$ and 90° with respect to the loading direction [27, 28]
- **Shear-out failure:** Shear-out failure is when a bolt is pulled through the end of the joint, see Figure 7.1 above. It is a ductile failure mode which is possible to occur when the distance between the hole and laminate edge is too small [27]. Contradictory to tension failure, shear-out failure tends to occur when there are too many plies oriented in the loading direction [28].
- **Bolt pulling through laminate:** The major structural limitation for bolts in laminates is the low through thickness strength of laminate [26]. It is therefore possible that the bolt is pulled through the laminate as illustrated in Figure 7.1. Bolt pull-through can occur when using countersunk bolts with too deep heads or when using shear headed bolts [28].
- **Bolt failure:** Unlike in metal joints, where the bolt is primarily loaded in tension and shear loads are transferred between the joined components, composite joints rely on the bolt to sustain bearing stresses. This makes bolt failure in bending important to consider in composite bolted joints. Bolt failure can occur when the bolt is too small for the laminate thickness, if there are gaps in the joint or if there is insufficient bolt clamp-up [28].

The fact that the above mentioned failure modes are abrupt or ductile is an important factor to consider in designing the composite joint. Abrupt failure modes are very sudden in behaviour and result in that the joint immediately after failure occurs becomes unable to carry any load which, depending on area of application, may lead to catastrophic consequences [27, 28]. Ductile failure modes act more slowly. The joint is also able to carry load until final failure [30]. Ductile failure modes are for these reasons the preferred failure modes in bolted composite joints. More specifically bearing failure is often the only acceptable failure mode to be designed against due to mentioned properties. It should however be noted that designing for this failure mode will result in a less than optimum joint strength [27, 28].

7.3 Design guidelines

The causes of the various failure modes mentioned in Section 7.2 indicates on corresponding measures to avoid them. This section is therefore intended to describe design guidelines which are mainly related to geometrical and laminate stacking sequence alterations but also at what type of bolt that should be used in order to make a bolted joint both predicable and strong.

7.3.1 Geometrical parameters

The influence of the geometrical parameters in composite joints can be, as mentioned in Section 7.2, of great importance for determining both if it will fail as well as how it will fail. The main geometrical parameters that are to be considered are defined in Figure 7.2.

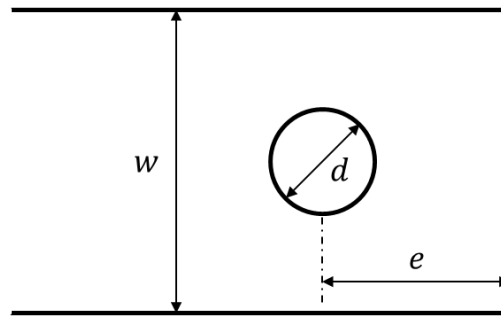


Figure 7.2: Illustration of geometrical parameters.

In Figure 7.2 d is the bolt diameter, e is the distance from the centre of the hole to the edge of the laminate and w is the width of the laminate. Research and investigations of the influence of these parameters have previously been carried out and defined for structural composites. The influence of the edge distance to diameter (e/d) and width to diameter (w/d) can be seen in Figure 7.3.

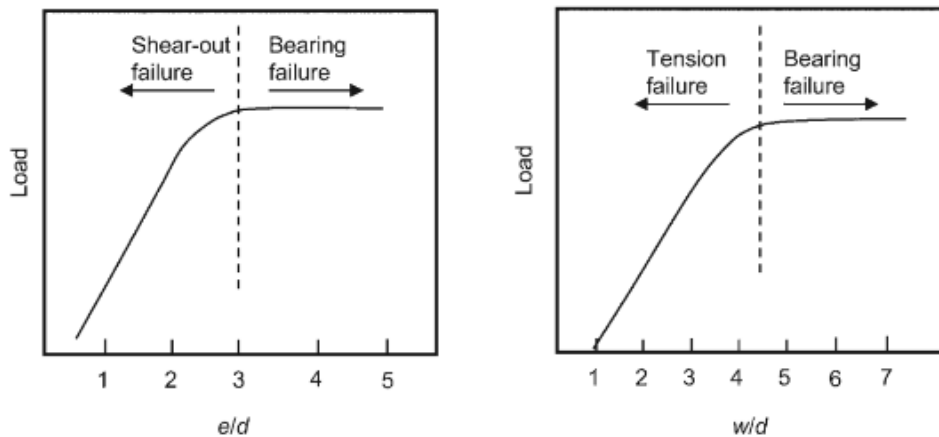


Figure 7.3: Effects of edge distances on laminate failure modes [28].

The numerical values and general behaviour of the shift between failure modes correspond well between literature [27, 28] and various investigations [30, 31]. The laminate layup does affect the numerical values for the transition between various modes and Figure 7.3 above is

for a quasi-isotropic layup. By using information of this type the possibility of avoiding unwanted failure modes is increased.

7.3.2 Laminate layup

The fact that the layup of the laminate has a significant effect on the failure modes of bolted joints is mentioned in Section 7.2 and has been investigated by researchers [30, 31]. The general conclusion is that laminates in bolted joints should not deviate greatly from a quasi-isotropic layup. This is also the case when examining guidelines for bolted joints developed for NASA and the composite materials handbook for the American department of defence [13, 14]. An illustration of allowable fibre layups is depicted in Figure 7.4.

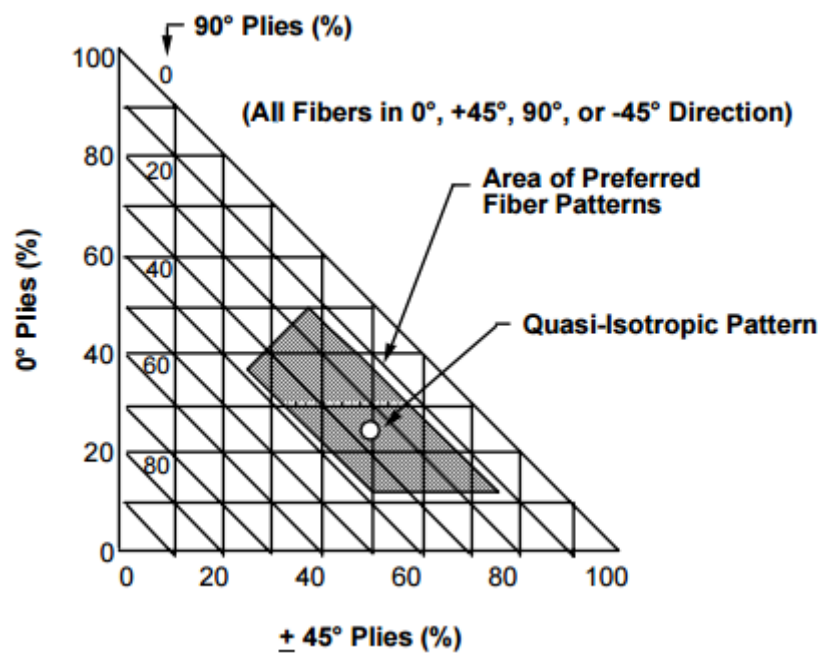


Figure 7.4: Suitable layups for bolted joints [14].

7.3.3 Bolt properties

The geometrical and material properties of the bolts are of significant importance. Since the joints are mainly to be designed against bearing failure, see Section 7.2, the bearing stress capabilities of the bolt is important. The bolt types that should be considered are mainly protruding head and countersunk bolts as illustrated in Figure 7.5.

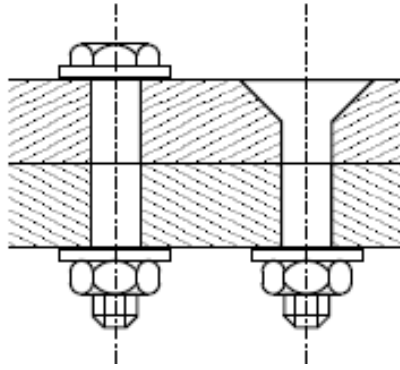


Figure 7.5: *Protruding head (left) and countersunk bolts (right) [30].*

A protruding head bolt offer greater bearing strength since it maximizes the length of the cylindrical bolt shank. It also allows for washers to be fitted against both head and nut creating a stress distribution that is less concentrated around the vicinity of the hole. Countersunk bolts are recommended to only be used when protruding head bolts cannot satisfy the requirements of the design [28], for example airplanes requiring smooth surfaces to lower drag. The advantage with these bolts is that they increase pull-through strength and delamination resistance thus allowing bolted joints to be used in thinner laminates [13]. The main disadvantages are that the bearing strength is decreased and a too deep countersink reduces both static strength and fatigue life of the joint.

7.4 Modelling of bolted joints

Unlike the main concept and the optimisation analysis, which uses Hypermesh as pre-processor and Optistruct as solver, the bolted joint analysis has been made using Abaqus as a solver whilst still using Hypermesh as the pre-processor. This is because the composite is to be modelled using a special script allowing composites to be modelled with shells in Hypermesh and converted to solid elements to capture out of plane stresses in the bolted joint. Abaqus allows implementation of subroutines (UMAT) which has been used to analyse the joint according to several failure criterion during the same solving procedure (Appendix G). The main differences in modelling for Abaqus compared to Optistruct are outlined in this section.

7.4.1 Material orientation

The method of aligning the laminate differs compared to the one described in Section 5. Abaqus uses a zone based modelling approach meaning that each area of the component that either has an individual surface or specific laminate layup needs to be handled individually with its own stacking sequence, material properties and ply orientation. Since each surface requires its own defined plies, layup and orientation it was therefore required to define a coordinate system for surfaces that are not parallel to each other as depicted in Figure 7.6.

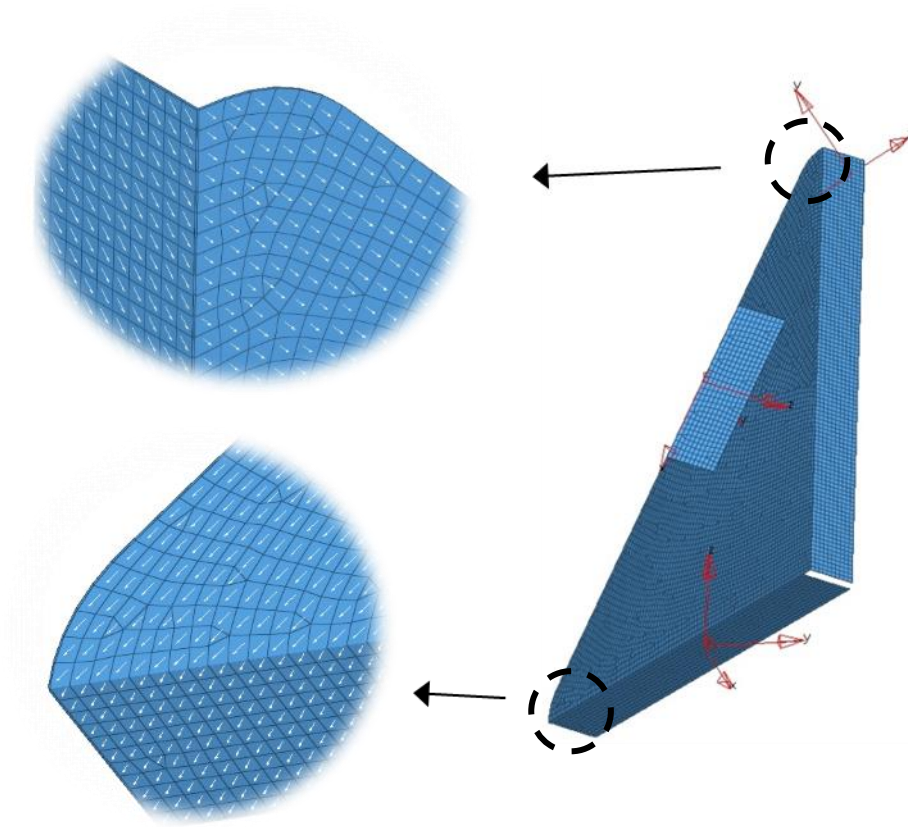


Figure 7.6: *Fibre orientations in parts of the corner. The images show how a specific layer is orientated along the geometry of the part.*

This method is needed to ensure control of the orientation of the plies on the entire model. In Figure 7.6 above each of the three defined coordinate systems are assigned to separately defined properties in the model which are then assigned to the elements making up the various parts of the corner. This method ensures control over the fibre orientation in the part.

7.4.2 Holes and washers

Until this point the model consists of shell elements and does not contain bolt holes. Since a bolted joint will result in local stress concentrations it becomes necessary to refine the mesh near the vicinity of the hole. This is to obtain an adequate stress distribution in order to analyse various failure criteria. The hole and the mesh of the surrounding washer are depicted in Figure 7.7.

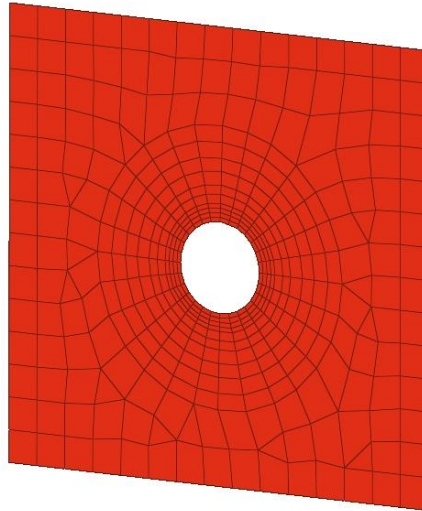


Figure 7.7: *Mesh refinement around hole.*

7.4.3 Laminates including solid elements

Once the holes are created and meshed the elements around the hole are to be converted from shell elements into solid elements. This has been done with the use of a script developed by Altair which does the shell to solid conversion and maintains the fibre orientation along previously defined coordinate systems. The main result of the procedure is depicted in Figure 7.8 below.

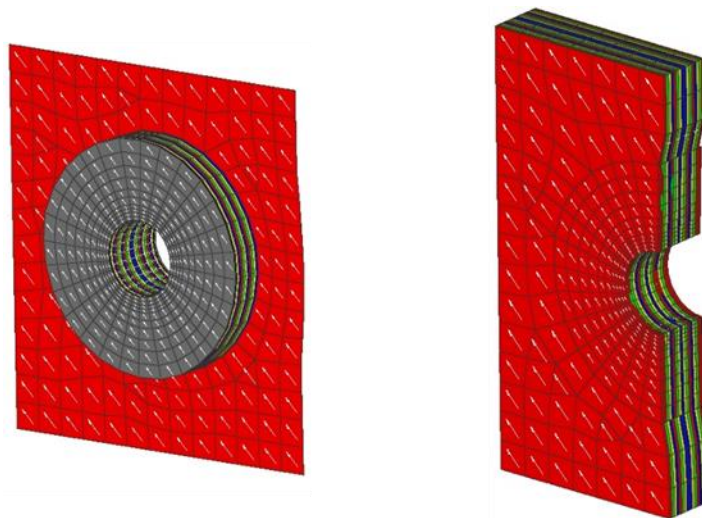


Figure 7.8: *Main component represented with shell elements and solid elements near the hole (left). True thickness representation (right).*

7.4.4 Element couplings

Using a combination of shell and solid elements to model the same physical component comes with more details to consider. Shell elements have six degrees of freedom (dof's), three in translation and three in rotation. Solid elements only have the three translational dof's. The

elements need therefore to be connected so that a realistic representation of the behaviour of the structure is achieved. To transfer the behaviour between shells and solids the most common way is to use shell to solid coupling. However this method requires manually coupling of all solid layers on all the bolts of the model to the corresponding shell elements. As seen in Figure 7.9 a technique where a shell mesh, coloured green in Figure 7.9 is generated on the outer envelope surface of the solid elements was used. These elements transferred the nodal information from the shells to the solids.

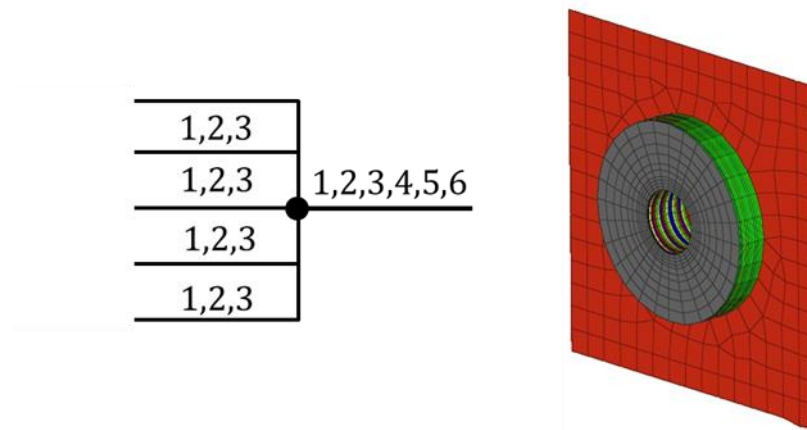


Figure 7.9: *Shell to solid principal (left) and used solution with shell meshing, coloured green, around solid layers (right).*

7.4.5 Bolts and contact

The types of bolts used in the model are protruding head bolts of size M14. The bolts have been modelled with a larger bolt-head diameter than conventional bolts and corresponding nut to account for the use of metallic washers in the joints, see Figure 7.10. The contact in the joint has been defined using the general contact function in Abaqus with contact surfaces defined as the entire bolts and nuts as well as the solid modelled laminates surrounding the bolt holes.

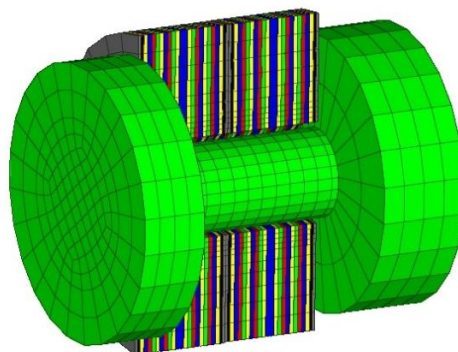


Figure 7.10: *Bolt with large head and nut positioned in holed laminates.*

7.4.6 Applied loading

The model with the bolted joints was then subjected to the distributed vertical load according to Section 2.2 as depicted in Figure 7.11 below. This load case was considered to assess the bolted joint simulation methodology.

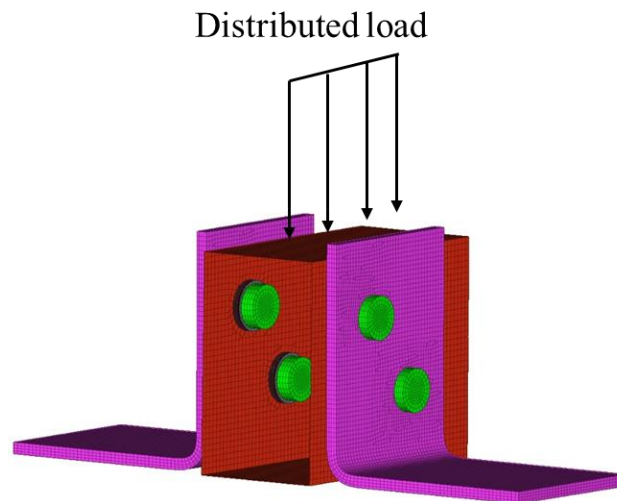


Figure 7.11: *Cut-out of model with bolted joints subjected to a distributed load. The purple brackets are attachments to the auxiliary frame.*

7.5 Failure analysis in composites

There are many criteria that can be used for determining failure in composites. These vary from 3D to 2D as well as developed from physical descriptions to empirical models. Failure criteria that are considered good in un-notched laminates might not necessarily be the most suitable in bolted laminates and FE-analysis. This section intends to describe the used methods for failure analysis in bolted joints regarding where to evaluate the stresses and what criteria to evaluate. Within this thesis the assumption is that the structure fails upon first ply failure.

7.5.1 Evaluation of holes in composites

Localised stress concentration damages will always occur in a bolted joint and creates demands for methods to describe the extent of the damage. In FE-analysis numerical discontinuities tend to occur in the vicinity of a hole making it an unsuitable area for evaluation. The stress field around holes in anisotropic materials is in general difficult to assess. Not only can the stress approach infinity near the vicinity of the hole but also be difficult to explain since the fibres are oriented differently and thus subjected to different types of stresses even though the fibres might be adjacent to each other.

There are several different methods for analysing composites with holes. One of the more simple methods is called the Point Stress Criterion (PSC) [25]. This criterion proposes that failure occurs when the stress at some characteristic distance away from the hole edge reaches the strength of the un-notched laminate according to

$$\sigma_y|_{x=R+d_0} = \sigma_0 \quad (7.1)$$

where σ_y is the stress, σ_0 is the maximum stress of the un-notched material, R is the hole radius and d_0 is the characteristic length as described in Figure 7.12 below.

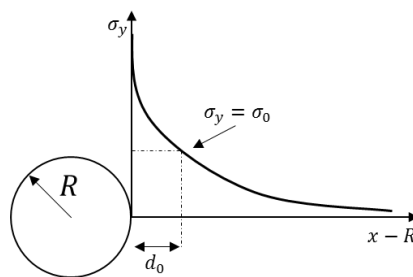


Figure 7.12: *Illustration of the Point Stress Criterion.*

The distance d_0 is a material parameter that has to be determined from testing. Several researchers [32, 33, 34] have all made efforts to determine this parameter analytically. It has however no physical interpretation and tests to find this value makes the criterion work in some but not all cases. There are however more sophisticated methods such as the Average Stress Criterion (ASC) and the Damage Zone Criterion (DZC) but these encounter similar problems with dependencies on physical tests to find necessary parameters. It should also be

mentioned that while all of these criteria have been considered good for tensile loading they have been deemed unsuitable for use in compressive loading [25].

In the present work the consideration regarding at what distance away from the hole vicinity to evaluate is taken into account but not according to the criteria mentioned in this section. Instead the behaviour close to the hole edge is used to evaluate the various failure criteria. The suitability of the mentioned criteria is left for future work when test data is available for a considered fibre composite material.

7.5.2 Tsai-Hill criterion

The Tsai-Hill failure criterion is a two dimensional criterion developed in order to take into account the interactions of combined loading. It is widely used and implemented into commercial FE-software for shell elements. It was developed based on the assumption that the von Mises yield criterion for isotropic materials could be generalised in order to be applicable to anisotropic materials [25]. The Tsai-Hill criterion predicts failure when

$$\left(\frac{\sigma_1}{\hat{\sigma}_1}\right)^2 - \frac{\sigma_1 \sigma_2}{\hat{\sigma}_1^2} + \left(\frac{\sigma_2}{\hat{\sigma}_2}\right)^2 + \left(\frac{\tau_{12}}{\hat{\tau}_{12}}\right)^2 = 1 \quad (7.2)$$

where $\sigma_{1,2}$ are the stresses in and transverse to the fibre direction, τ_{12} is the in plane shear stress and the corresponding values in the denominator are the corresponding strength limitations. This criterion does not separate tension from compression which is fundamental in fibre composite analysis and needs to be accounted for. When implementing this criterion it was therefore necessary to apply the following into the UMAT subroutine

$$\begin{cases} \hat{\sigma}_1 = \hat{\sigma}_{1t}, & \sigma_1 \geq 0 \\ \hat{\sigma}_1 = \hat{\sigma}_{1c}, & \sigma_1 < 0 \end{cases} \quad \begin{cases} \hat{\sigma}_2 = \hat{\sigma}_{2t}, & \sigma_2 \geq 0 \\ \hat{\sigma}_2 = \hat{\sigma}_{2c}, & \sigma_2 < 0 \end{cases} \quad (7.3)$$

where $\hat{\sigma}_{1t}, \hat{\sigma}_{1c}$ are the tensile and compressive stress limits in the fibre direction and $\hat{\sigma}_{2t}, \hat{\sigma}_{2c}$ are the corresponding transverse to the fibre direction.

7.5.3 Tsai-Wu criterion

This is a criterion similar to the Tsai-Hill criterion. It is a quadratic criterion and is widely used due to its simple implementation and mathematical simplicity. The equation states the following when failure occurs

$$\frac{\sigma_1^2}{\hat{\sigma}_{1t}\hat{\sigma}_{1c}} + \frac{\sigma_2^2}{\hat{\sigma}_{2t}\hat{\sigma}_{2c}} + \left(\frac{\tau_{12}}{\hat{\tau}_{12}}\right)^2 + 2F_{12}\sigma_1\sigma_2 + \frac{\sigma_1}{\hat{\sigma}_{1t}} - \frac{\sigma_1}{\hat{\sigma}_{1c}} + \frac{\sigma_2}{\hat{\sigma}_{2t}} - \frac{\sigma_2}{\hat{\sigma}_{2c}} = 1 \quad (7.4)$$

where the interaction term F_{12} needs to be determined through biaxial testing of the material [25]. The term is defined as

$$F_{12} = F_{12}^* \sqrt{\frac{1}{\hat{\sigma}_{1t}\hat{\sigma}_{1c}} \frac{1}{\hat{\sigma}_{2t}\hat{\sigma}_{2c}}} \quad (7.5)$$

where $-1 < F_{12}^* < 1$ is needed in order to for the criterion to represent an elliptical curve. Since accurate biaxial tests are difficult to perform the value of F_{12} is often arbitrarily set to zero in practice and several researchers [35] have found the term to be insignificant and suggested that it should be set equal to zero. This is therefore done in this thesis in order to avoid uncertainties and due to the absence of test data.

A benefit with the Tsai-Wu criterion is that it can, unlike the Tsai-Hill criterion, be used directly without a need for modification depending on the stress signs. The drawback is that it does not explicitly identify failure mechanisms making it difficult for the engineer to read into the meaning of the results. It should be noted that both the Tsai-Hill and Tsai-Wu criteria are essentially empirical models adapted by curve fitting to experimental observations and can therefore not identify the specific failure modes.

7.5.4 Yamada-Sun criterion

The Yamada-Sun criterion [36] is based on the fact that the main concern is the first ply failure of a whole laminate and the importance of the shear stresses on the plies within the laminate. It assumes that when a single lamina fails a total failure of the whole laminate is to occur due to breaking of fibres or layer separation due to shear failure. It has shown good agreement with experimental results [32]. The criterion states

$$\left(\frac{\sigma_1}{\hat{\sigma}_1}\right)^2 + \left(\frac{\tau_{12}}{\hat{\tau}_{12}}\right)^2 = l^2 \quad \text{and} \quad \begin{cases} l \geq 1 & \text{failure} \\ l < 1 & \text{no failure} \end{cases} \quad (7.6)$$

where the longitudinal strength $\hat{\sigma}_1$ has been applied as tensile or compressive strength based on the sign of the σ_1 stress component as described in (7.3). A significant advantage with the Yamada-Sun criterion is that it requires few material related strength parameters.

7.5.5 Hashin 3D criterion

This failure criterion is (along with Puck and Cuntze) a criterion intended to take into account the actual physical behaviour during fracture. The foundation is in that since each failure mode is different it has to be modelled and compared against a different criterion. The Hashin 3D criterion [37] states the following for fibre failure (F_f)

$$F_f = \begin{cases} \left(\frac{\sigma_1}{\hat{\sigma}_{1t}}\right)^2 + \frac{1}{\hat{\tau}_{12}^2}(\tau_{12}^2 + \tau_{13}^2) & \sigma_1 \geq 0 \\ \left(\frac{\sigma_1}{\hat{\sigma}_{1c}}\right)^2 & \sigma_1 < 0 \end{cases} \quad (7.7)$$

where τ_{13} is the out of plane shear stress and is the difference between the 2D and 3D criterion. The criterion for matrix failure is

$$F_m = \begin{cases} \frac{(\sigma_2 + \sigma_3)^2}{\hat{\sigma}_{2t}^2} + \frac{(\tau_{12}^2 - (\sigma_2 \sigma_3))}{\hat{\tau}_{23}^2} + \frac{\tau_{12}^2 - \tau_{13}^2}{\hat{\tau}_{13}^2} & (\sigma_2 + \sigma_3) \geq 0 \\ \frac{(\sigma_2 + \sigma_3)}{\hat{\sigma}_{2c}} \left(\left(\frac{\hat{\sigma}_{2c}}{2\hat{\tau}_{23}^2} \right)^2 - 1 \right) + \frac{(\sigma_2 + \sigma_3)^2}{4\hat{\tau}_{23}^2} + \frac{\tau_{23}^2 - (\sigma_2 \sigma_3)}{\hat{\tau}_{23}^2} + \frac{\tau_{12}^2 + \tau_{13}^2}{\hat{\tau}_{12}^2} & (\sigma_2 + \sigma_3) < 0 \end{cases} \quad (7.8)$$

where the first equation considers matrix failure in tension and the second deals with the corresponding in compression. The equations for the Hashin criterion illustrate the previous

point. The different failure mechanisms are accounted for since the actual criterion (and not just the parameter values) is changed based on the type of loading.

Similar to previous criteria failure occurs when F_f or F_m equals unity.

7.5.6 Puck criterion

The Puck 3D failure criterion [38] is an interactive criterion based on an assumption that failure occurs at a fracture plane which is inclined with an angle θ against the standard material plane and is caused by normal and shear stresses. It separates between fibre and inter fibre failure. The fibre failure criterion is

$$f_{E(FF)} = \begin{cases} \frac{1}{\hat{\varepsilon}_{1t}} \left(\varepsilon_1 + \frac{\nu_{f12}}{E_{f1}} m_{\sigma f} \sigma_2 \right) & \text{for } (...) \geq 0 \\ \frac{1}{\hat{\varepsilon}_{1c}} \left| \left(\varepsilon_1 + \frac{\nu_{f12}}{E_{f1}} m_{\sigma f} \sigma_2 \right) \right| & \text{for } (...) < 0 \end{cases} \quad (7.9)$$

where $\hat{\varepsilon}_{1t}$ and $\hat{\varepsilon}_{1c}$ are the maximum longitudinal tensile and compressive strains respectively, ν_{f12} and E_{f1} are the poisons ratio and the Young's modulus of the ply in the fibre direction and $m_{\sigma f}$ is a stress magnification factor that is recommended [37, 38] to be set equal to 1.1 for carbon fibre composites and has been used herein. The Puck criterion is mostly considered due to its well-developed inter fibre failure criterion which basically is matrix failure. The assumption is that fractures are only created due to the stresses that act on the fracture plane which can be inclined by -90° to 90° against the standard material plane as illustrated in Figure 7.13 below.

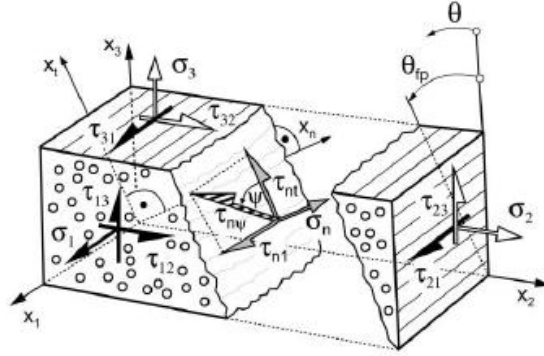


Figure 7.13: Fracture plane example shown relative to standard material plane [39].

The normal and shear stresses (transverse and parallel to the fibres) acting on the inclined plane, σ_n , τ_{nt} and τ_{nl} are calculated by tensor transformations according to the following

$$\begin{cases} \sigma_n(\theta) = \sigma_2 \cos^2(\theta) + \sigma_3 \sin^2(\theta) + 2\tau_{23} \sin(\theta)\cos(\theta) \\ \tau_{nt}(\theta) = (\sigma_3 - \sigma_2) \sin(\theta) \cos(\theta) + \tau_{23}(\cos^2(\theta) - \sin^2(\theta)) \\ \tau_{nl}(\theta) = \tau_{31} \sin(\theta) + \tau_{21} \cos(\theta) \end{cases} \quad (7.10)$$

which meant that a looping procedure needed to be implemented in order to determine the maximum value for the stress components. The failure criterion for matrix failure, $f_{E(IFF)}$, thus becomes the following

$$f_{E(IFF)} = \begin{cases} \sqrt{\left[\left(\frac{1}{R_{\perp}} - \frac{P_{\perp\psi}^+}{R_{\perp\psi}}\right)\sigma_n(\theta)\right]^2 + \left(\frac{\tau_{nt}(\theta)}{R_{\perp\perp}}\right)^2 + \left(\frac{\tau_{nl}(\theta)}{R_{\perp\parallel}}\right)^2 + \frac{P_{\perp\psi}^+}{R_{\perp\psi}}\sigma_n(\theta)} & \text{for } \sigma_n \geq 0 \\ \sqrt{\left(\frac{\tau_{nt}(\theta)}{R_{\perp\perp}}\right)^2 + \left(\frac{\tau_{nl}(\theta)}{R_{\perp\parallel}}\right)^2 + \left[\frac{P_{\perp\psi}^-}{R_{\perp\psi}}\sigma_n(\theta)\right]^2} + \frac{P_{\perp\psi}^-}{R_{\perp\psi}}\sigma_n(\theta) & \text{for } \sigma_n < 0 \end{cases} \quad (7.11)$$

where R_{\perp} is the failure resistance in the normal direction against the fibres, $R_{\perp\psi}$ and $R_{\perp\parallel}$ are the shear resistances and the $P_{\perp\psi}^+$ and $P_{\perp\psi}^-$ are slope parameters representing effects of internal friction. The parameters for equation (7.11) are determined and implemented according to the following

$$R_{\perp} = \hat{\sigma}_{2t} \quad R_{\perp\parallel} = \hat{\tau}_{12} \quad R_{\perp\perp} = \frac{\hat{\sigma}_{2c}}{2(1 + P_{\perp\perp}^-)} \quad (7.12)$$

and

$$\frac{P_{\perp\psi}^+}{R_{\perp\psi}} = \frac{P_{\perp\perp}^+}{R_{\perp\perp}} \cos^2(\psi) + \frac{P_{\perp\parallel}^+}{R_{\perp\parallel}} \sin^2(\psi) \quad \frac{P_{\perp\psi}^-}{R_{\perp\psi}} = \frac{P_{\perp\perp}^-}{R_{\perp\perp}} \cos^2(\psi) + \frac{P_{\perp\parallel}^-}{R_{\perp\parallel}} \sin^2(\psi) \quad (7.13)$$

where the parameters $P_{\perp\parallel}^+$, $P_{\perp\parallel}^-$, $P_{\perp\perp}^+$ and $P_{\perp\perp}^-$ are special Puck parameters which require multiaxial testing. However a recommendation is provided by Puck [39] that the parameters should be set to the following values

$$P_{\perp\parallel}^+ = 0.35 \quad P_{\perp\parallel}^- = 0.30 \quad P_{\perp\perp}^+ = 0.30 \quad P_{\perp\perp}^- = 0.30 \quad (7.14)$$

which have been used in the present work.

7.5.7 Cuntze criterion

The Cuntze failure criterion [40] uses a similar approach as Puck but assumes that probabilistic and mechanical interactions cannot be clearly distinguished thus resulting in interactions between failure modes [41]. Both assume that failure can occur due to the stresses on an inclined fracture plane but while the Puck criterions needs to loop the stresses over an inclination angle of the plane θ Cuntze uses invariants formulated according to the following

$$\begin{aligned} I_1 &= \sigma_1 & I_2 &= \sigma_2 + \sigma_3 & I_3 &= \tau_{12}^2 + \tau_{13}^2 & I_4 &= (\sigma_2 - \sigma_3)^2 + 4\tau_{23}^2 \\ I_5 &= (\sigma_2 - \sigma_3)(\tau_{13}^2 - \tau_{12}^2) - 4\tau_{23}\tau_{13}\tau_{12} \end{aligned} \quad (7.15)$$

These invariants are then used to formulate the failure criteria for the different failure modes. Similarly to both Puck and Hashin, Cuntze separates between fibre failure and matrix failure but does also distinguish between the types of fracture. The following conditions for fibre failure (FF) and inter fibre failure (IFF) have been used

$$\begin{aligned}
FF1 &= \frac{I_1}{\hat{\sigma}_{1t}} = 1 \\
FF2 &= \frac{-I_1}{\hat{\sigma}_{1c}} = 1 \\
IFF1 &= \frac{I_2 + \sqrt{I_4}}{2\hat{\sigma}_{2t}} = 1 \\
IFF2 &= \frac{I_3^{3/2}}{\hat{\tau}_{12}^3} + b_{\perp\parallel} \frac{I_2 I_3 - I_5}{\hat{\tau}_{12}^3} = 1 \\
IFF3 &= (b_{\perp}^{\tau} - 1) \frac{I_2}{\hat{\sigma}_{2c}} + \frac{b_{\perp}^{\tau} I_4 - b_{\perp\parallel}^{\tau} I_3}{\hat{\sigma}_{2c}^2} = 1
\end{aligned} \tag{7.16}$$

where $b_{\perp\parallel}$, b_{\perp}^{τ} and $b_{\perp\parallel}^{\tau}$ are curve parameters that should be determined from multiaxial tests. However Cuntze [40] have managed to determine bounds for the values of these which have been used in this present work. The used parameter values are listed below

$$b_{\perp\parallel} = 0.1 \quad b_{\perp}^{\tau} = 1.1 \quad b_{\perp\parallel}^{\tau} = 0.1 \tag{7.17}$$

which are within the determined bounds and recommended by Cuntze as a good approach [40]. Figure 7.14 provides a visual representation of the failure modes.

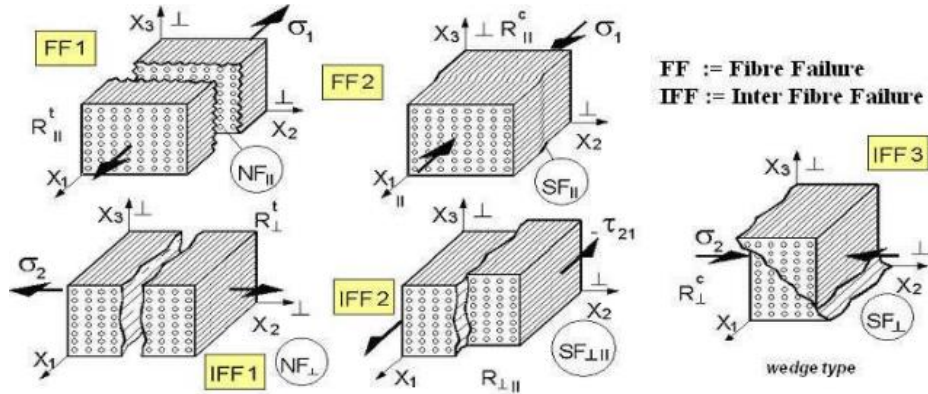


Figure 7.14: Illustration of failure modes according to Cuntze [40].

7.6 Results

The anisotropic behaviour was observed when loading the bolted joint. As an example the failure index variation according to the Puck matrix criterion can be seen in Figure 7.15 below.

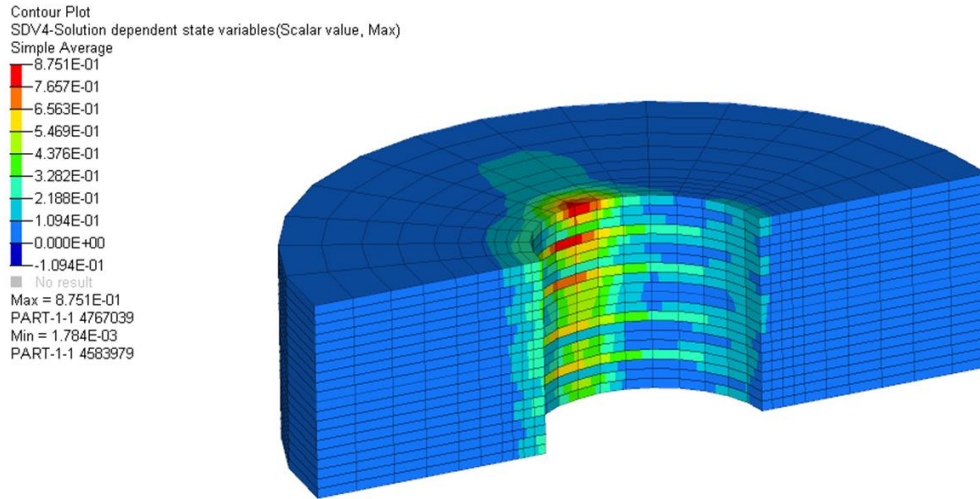


Figure 7.15: *Puck matrix criterion variation within composite laminate.*

A more detailed example can be seen in Figure 7.16 where the Puck matrix criterion variation within a 45° layer is illustrated.

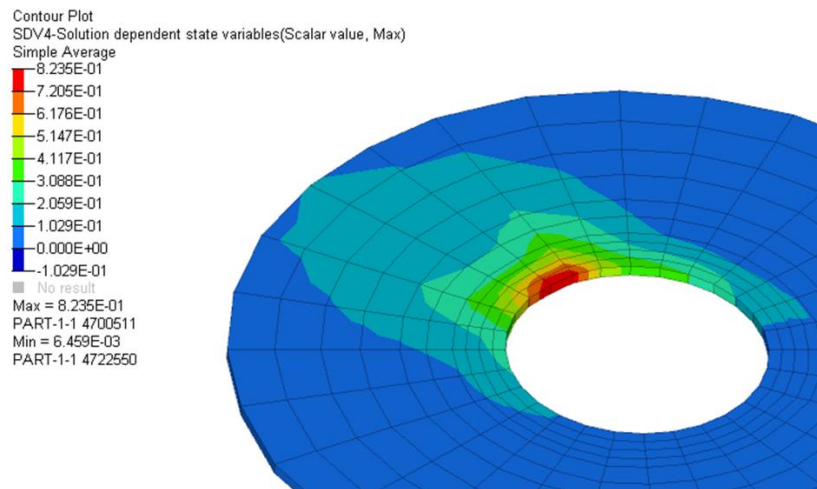


Figure 7.16: *Puck matrix criterion in a 45° oriented layer.*

Similarly Figure 7.17 displays the variation of the Puck matrix failure criterion for the adjacent -45° layer.

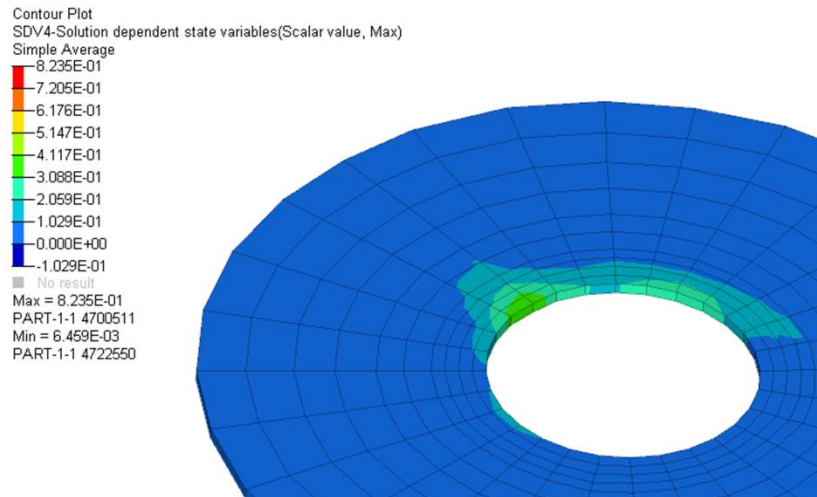


Figure 7.17: Puck matrix criterion in a -45° oriented layer.

A distinction was made between different failure criteria when evaluating the results. In Figure 7.18-7.20 failure indices are displayed in terms of their typical variations with the distance from the hole edge obtained from the analyses.

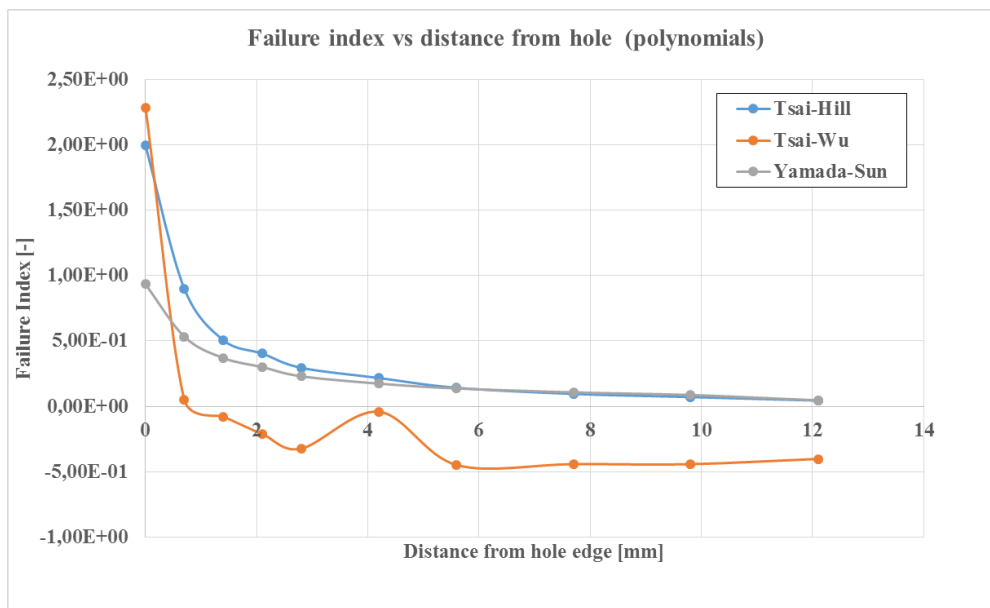


Figure 7.18: Failure index variation with distance from hole edge.

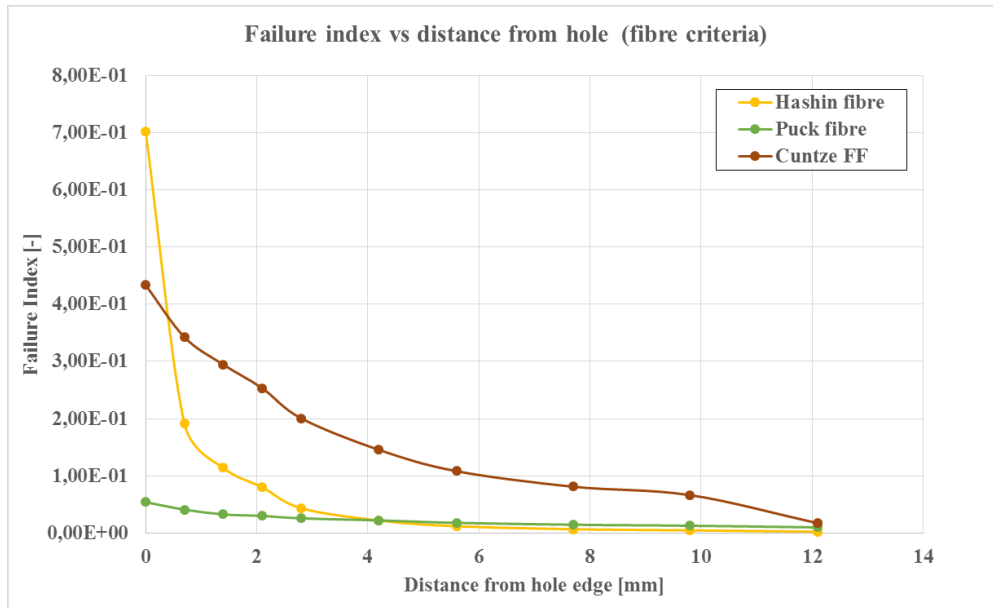


Figure 7.19: *Fibre failure index variation with distance from hole edge.*

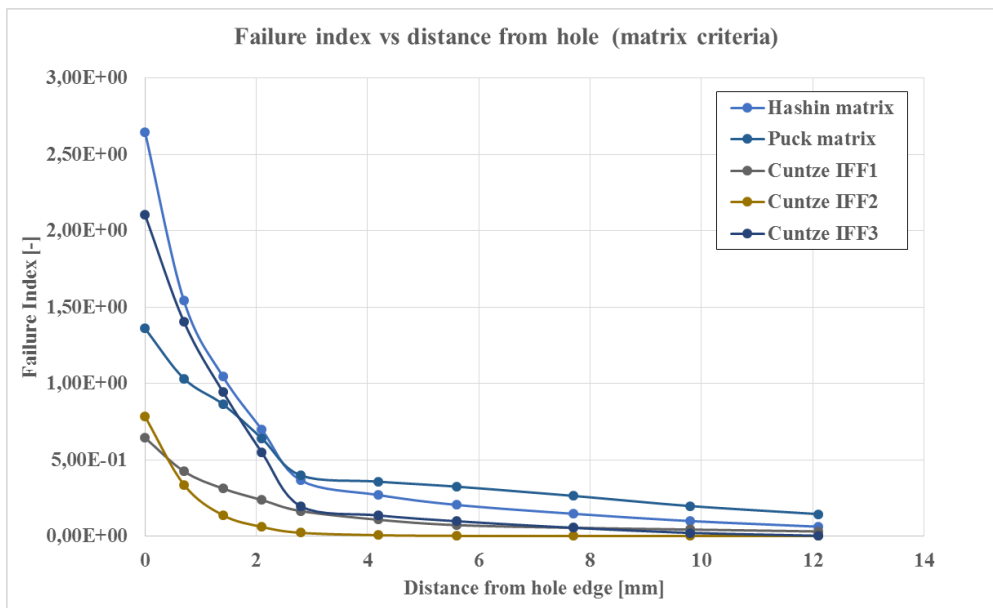


Figure 7.20: *Matrix failure index variation with distance from hole edge.*

7.7 Discussion of bolted joint analysis

7.7.1 Failure criterion analysis

Effects of discontinuities near the hole edge did not become extremely high as could be expected from literature [25] but can be seen throughout the results for various layers and cannot be neglected thus making it unsuitable to analyse the stresses at the hole edge. The used algorithm for contact between bolt and laminate edges performed well. There is however room for improvement and more elaborate contact definitions will most likely decrease the effect of edge discontinuities further.

The general conclusion from the results is that failure in the analysed bolted joints are highly dominated by matrix failure. The matrix failure modes for the Puck and Hashin criterion are in general the highest ones throughout the analyses showing the significance to account for out of plane stresses by having three-dimensional matrix criteria during bolted joint analyses. When observing the failure indices (FI) of these criteria along the distance from the hole edge they also show an exponentially stable behaviour which is in agreement with notch fracture theories [25]. The Cuntze IFF criterion clarifies the particular failure modes more distinctly than both Puck and Hashin matrix criteria making it very desirable for engineering usage. Although it originates from the Puck criterion in its assumptions it states considerably lower FI throughout the analysed layers.

For fibre failure the Puck criterion differs significantly from the others. The Puck criterion consistently gives the by far lowest FI and thus predicts fibre failure to never be close to occur. The main difference between Puck and the other criteria considered for fibre failure (Cuntze, Hashin, Yamada-Sun) is that Puck is a strain based fibre failure criterion. When comparing the stresses and strains in the considered bolts the stresses are one to two orders of magnitude closer to failure according to the failure index (using maximum stress/strain criterions) comparing to the strains. An explanation could be that the geometrical setup with an metallic L-plate on one side and large washers on the other as well as the applied loads (pretension and vertical compressive load) may lead to a scenario where stresses are more or less reliable. Another area of uncertainty is the value of the constant $m_{\sigma f}$ since it has not been investigated in this type of application.

When comparing the other fibre failure criteria similar behaviour can be found in Yamada-Sun and Cuntze. Unlike Cuntze FF which is the same as the maximum stress criterion applied in the fibre direction Yamada-Sun takes into account the in-plane shear stresses as well and the significance of these can clearly be seen closer to the hole edge. The Yamada-Sun criterion always provides a more conservative value than Cuntze but becomes very similar as the distance from the hole increases. The Hashin criterion for fibre failure differs from these two slightly as it accounts for out of plane shear stresses in tension as well as being quadratic in its formulation. The results indicates this criterion to be more sensitive to effects of discontinuities near the hole edge as well as having a more extreme behaviour in exponential decrease with distance from the hole.

Tsai-Hill resembles the behaviour of Yamada-Sun but with less conservative results. Similar to the Hashin fibre failure criterion it is quadratic in its formulation thus allowing more extreme behaviour in terms of variation with the distance from the hole edge.

The results of Tsai-Wu are difficult to interpret. Tsai-Wu almost always lead to negative values with increasing distance to the hole edge making it difficult to make judgements based

on the value and behaviour of this criterion. It is intended to work similarly to Tsai-Hill but its formulation allows negative FI results for certain load cases with compressive normal stresses along and transverse to the fibre direction. For example in an element the stresses were $\sigma_1 = -19.6$ MPa, $\sigma_2 = -43.9$ MPa, $\tau_{12} = 1.9$ MPa so that $FI_{Wu} = -0.43$. Unlike the other criteria it did not converge in an exponentially stable manner but changed from decreasing to increasing along the distance from the hole edge. An alteration was made by setting F_{12}^* to -0.5 which is commonly used and also recommended [25, 35] as well but with no change in the results.

Both Tsai-Hill and Tsai-Wu are, as mentioned in Section 7.5 are not physically based but developed using empirical test results. This means that they are formulated in a way that is primarily adapted for unnotched laminates. Also since they do not separate between failure modes the main conclusion is that it is probably best to use a physically based criteria for fibre and matrix failure separately in order to both capture and explain the mechanical integrity in a bolted joint for real life applications such as engineering FE-analysis.

It should however be mentioned that all of the indications and results need to be compared by actual testing on a similar setup in order to create a reference to compare against. Practical testing has not been included in this thesis. The work has been primarily directed towards setting up a model and determine a suitable methodology for analysing bolted joints in composites.

7.7.2 Modelling

The estimated workload can in many cases be considerable. The effort to set up a working FE-model with solid laminates and bolted joints with realistic contact mechanics and boundary conditions are an order of magnitude higher than implementing the various failure criteria. The Hypermesh toolbox used for the modelling makes it possible to model each lamina using solid elements but the amount of additional work currently needed to finalise the model for solving and post processing makes it unsuitable (in its current form) for large scale engineering applications.

The estimated workload in order to implement each criterion can differ significantly depending on the users experience of the selected coding language and on the amount of additional parameters that need to be obtained for implementation. The polynomial criteria (Tsai-Hill, Tsai-Wu, Yamada-Sun) were simply formulated and required standardised material data (apart from the F_{12}^* in Tsai-Wu) and therefore allowed a straightforward method for implementation. In contrast, the Puck criterion required more elaborate coding in order to loop over the angles of the fracture plane as well as needing more than standard parameters for implementation. The computational time is considered negligible.

It should be noted that the conclusions on workload and effort are based on this present work where the authors had to start from scratch with newly developed and thus previously unused modelling methodology and not selected failure criteria. For engineering purposes the used methods and the developed UMAT subroutine can be reused and adapted for any model with a much lower effort than stated here.

7.8 Conclusions of bolted joint analysis

The following conclusions were made from the bolted joint analysis:

- A working methodology for modelling bolted joints in composite structures and analysing several failure criteria has been developed. A new toolbox in Hypermesh was used and is considered to be suitable for modelling bolted joints in composites. It is however in need of development in order to achieve a higher level of automatization in the procedure for commercial engineering usage.
- Conducting an analysis of bolted joints is a complicated task. The used failure criteria, apart from Tsai-Wu, are considered as applicable for implementation in engineering applications but to find the most suitable criterion further investigation and experimental testing is required as the criteria are not in agreement.
- Effects of discontinuities need to be accounted for by evaluating the stress state at a small distance from the hole edge and further criteria are in need of development to establish an inspection point.
- The Puck and Hashin criteria are considered to be the best for describing inter fibre failure which was the dominating failure mode in the bolted joints. These criteria are also physically based which implies a wide area of use in contrast to empirical criteria that only valid in similar situations as the calibration during their development.
- The Yamada-Sun criterion is considered well developed for use as a failure criterion due to its stable behaviour and results that are close to more elaborate criteria whilst still being conservative. It is considered suitable for use as both a complete criterion or more probably in conjunction with more elaborate three dimensional matrix criteria. Fibre failure tends to have a smaller impact on the mechanical integrity of the bolt. Therefore a simple criterion is sufficient.
- Tsai-Wu and Puck fibre failure criteria are considered as unsuitable for use in bolted joint analysis due to the fact that their lack of capability to produce interpretable results in compressive-compressive loading which is prone to occur in bolted joints.
- Computational time depends entirely on the model and not the criteria implemented in the UMAT subroutine.

8. Impact analysis

One of the load cases relevant for a timber bolster is the impact from a log being aligned by hitting the log against the bolster. The load case is visualised in Figure 8.1 below.

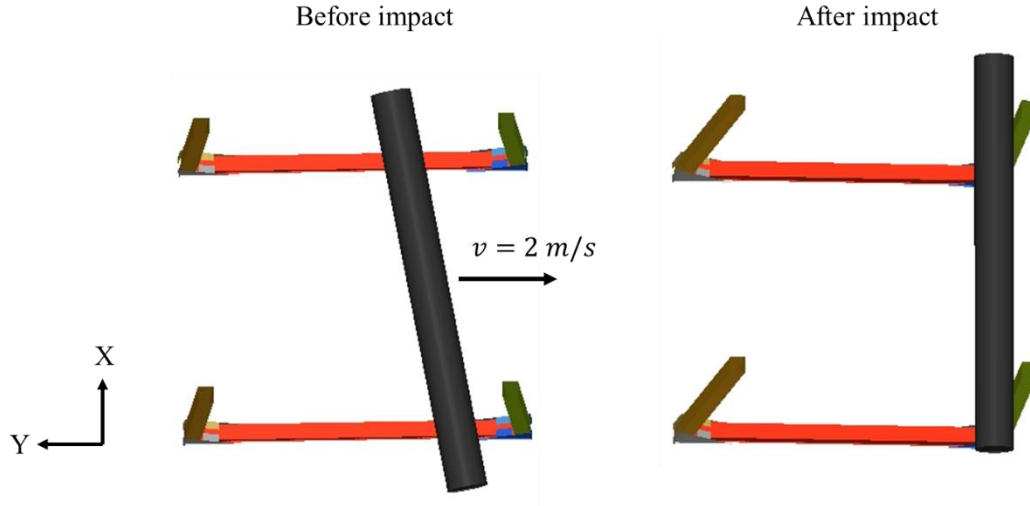


Figure 8.1: Alignment of log by hitting it towards timber bolsters.

8.1 Method

8.1.1 Analytical approach

Initially the impact was analysed using an energy analysis in order to find the displacement an impact causes. The energy calculation assumes that the kinetic energy from the log fully transforms into potential energy in the timber bolster at impact. The kinetic energy in a 190 kg log travelling at 2 m/s can be calculated via

$$KE = \frac{mv^2}{2} \quad (8.1)$$

where m is the mass and v is the velocity. The potential energy in the timber bolster is calculated by

$$PE = \frac{kx^2}{2} \quad (8.2)$$

where x is the displacement of the vertical beams and k is the stiffness. The stiffness was obtained by applying a point load and measuring the displacement at the top of the bolster in a FE-calculation. By combining (8.1) and (8.2) the displacement of the bolster due to the impact can be calculated via

$$x = \sqrt{\frac{mv^2}{k}} \quad (8.3)$$

which is later compared against simulations. Finally the force acting on the bolster was calculated according to

$$F_R = kx \quad (8.4)$$

which was compared with a simulation.

8.1.2 Impact simulation

Within this thesis a dynamic impact simulation was done using Abaqus Explicit [42]. Impact simulations were made based on several simplifications. Possibly the most significant simplification was the use of 2D elements. The impact was assumed to occur with a log traveling at a constant speed. The energies were monitored during the simulation, the total energy should be nearly constant during the simulation and before the log hits the bolster the kinetic energy of the log as calculated in equation (8.1) should coincide with the total energy. Reaction forces and the displacement of the bolster was also compared with results from the energy equation to verify the calculations.

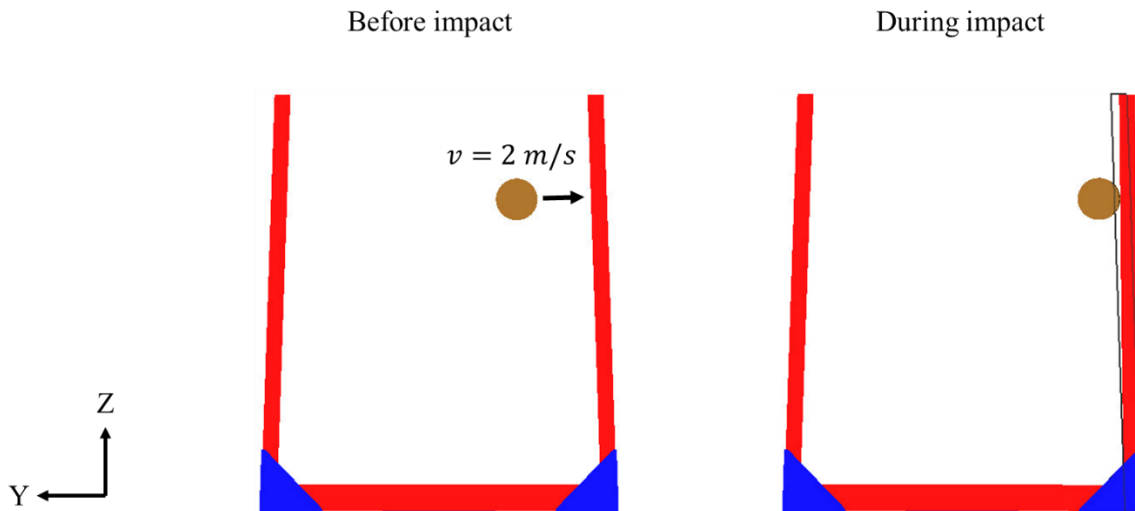


Figure 8.2: Log position before and during impact, including deformed and undeformed shape.

8.2 Results

The energies variation with time is displayed in Figure 8.3 below. The total energy is denoted ETOTAL and the kinetic energy of the log ALLKE. The reaction forces and displacements together with relevant energies are presented in Table 8.1.

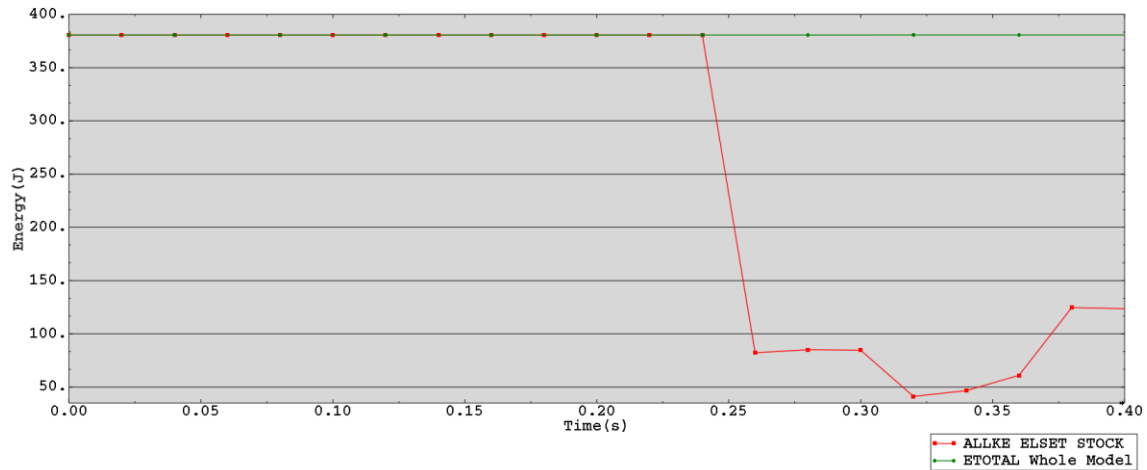


Figure 8.3: Total energy of the system and kinetic energy of the log as function of time Impact occurs after approximately 0.25 seconds.

Table 8.1: Comparison between analytical calculations and simulation.

Parameter	Analytical	Simulation
KE [J]	380	381
x [m]	0.0687	0.0473
k [kN/m]	161	161
F_R [kN]	11	20-30

8.3 Discussion of impact analysis

The dynamic behaviour of the bolster caused by an impact is difficult to predict. Several different simulations were made and the model was sensitive to small changes in for example initial velocity. For certain simulations the movement of the bolster looked almost as if a natural frequency was exited and the movement was very difficult to predict. Regarding the accuracy of the simulation its seen that the displacement differs but not as much as the forces. A possible explanation is the dynamic behaviour that is not considered in the analytical calculations. The forces also varies significantly at impact and shortly after due to the dynamics which makes it difficult to estimate the reaction force to be used when comparing with the energy equation.

A possible simplification would be to find the static load giving the same displacement and then use the static simulation to find failure indices. This would not be perfect but would be a good substitute for low velocity impacts.

In summary this chapter shows a possible approach to the impact analysis but a more detailed study is needed. For future work the recommendation is to use 3D elements and cohesive elements between each layer, a costly method but if done properly one can analyse failure and the accuracy will increase significantly. The implementation of a progressive failure model would also be of interest.

9. Concluding remarks

The purpose of this thesis was to use simulation and optimisation driven design to develop a fibre composite component. Overall the simulations using state of the art software, Hyperworks and Abaqus, was helpful when analysing anisotropic materials.

The methodology used for optimisation indicates that the potential weight saving is significant. In particular for the forestry industry a potential business case for composite materials was found. To further develop the optimisation methodology a more detailed study on the designs effect on manufacturing cost is needed.

One conclusion from the concept study is that all design features such as manufacturing, geometry and material selection are dependent on each other. This makes the concept selection more difficult.

A methodology for bolt analysis has been developed and computationally assessed. It is however time consuming using todays software tools and not developed for large scale analysis of bolts in composites. Further work is required regarding failure criteria and automatization of post processing. Finally the methodology should be verified against experiments.

References

- [1] Efundu, "Composite lamina principal," Efundu, [Online]. Available: http://www.efunda.com/formulae/solid_mechanics/composites/comp_lamina_principal.cfm. [Accessed 18 06 2016].
- [2] C. Löfroth and G. Svenson, "ETT-Modulsystem för skogstransporter," Skogsforsk, Uppsala, 2012.
- [3] G. Andersson and M. Frisk, "Stora Lastbilar ger goda miljöeffekter," Skogsforsk, 2013. [Online]. Available: <http://www.skogforsk.se/kunskap/kunskapsbanken/2013/Skogsbrukets-transporter-20101/>. [Accessed 05 06 2016].
- [4] G. Mercier, "FPInnovations Meets with Industry at DEMO International," Logging and Sawmilling Journal, 2012. [Online]. Available: http://forestnet.com/LSJissues/nov_dec2012/edge.php. [Accessed 25 05 2016].
- [5] Convestro AG, "Convestro, Baydur PUL 2500," Convestro AG, 2012. [Online]. Available: <http://www.polyurethanes.covestro.com/en/Products/Polyurethane-Systems/BAYDUR/ProductList/201312050324/BAYDUR-PUL-2500>. [Accessed 05 06 2016].
- [6] "Urethane Pultrusions," 2011. [Online]. Available: http://urethaneblog.typepad.com/my_weblog/2011/02/urethane-pultrusions.html. [Accessed 05 06 2016].
- [7] P. Vaillancourt, "Lighten Up: Carry More," Wood Business, 2012. [Online]. Available: <http://www.woodbusiness.ca/harvesting/lighten-up-carry-more>. [Accessed 05 06 2016].
- [8] S. Jacob, "Polyurethane composite used in timber trailer," Materials Today, 2011. [Online]. Available: <http://www.materialstoday.com/composite-applications/news/polyurethane-composite-used-in-timber-trailer/>. [Accessed 05 06 2016].
- [9] Exte Fabriks AB, "Produkter A-serien," Exte Fabriks AB, [Online]. Available: <http://www.exte.se/produkter/landsvagsprodukter/a-serien>. [Accessed 10 02 2016].
- [10] Exte Fabriks AB, "A-Serien Broschyr," Exte Fabriks AB, [Online]. Available: <http://www.exte.se/produkter/a-serien> <http://www.exte.se/upl/files/108335.pdf>. [Accessed 10 02 2016].
- [11] Vägverket, Fordonsavdelningen, "Säkring av last," Vägverket, Stockholm, 1999.
- [12] B. Hedlund. [Online]. Available: http://www.bengthedlund.se/0708/mobilinfo/lastsakring_start.htm. [Accessed 10 03 2016].

- [13] Departement of Defense, "Composite Materials Handbook Volume 3," American Departement of Defense, 2002.
- [14] J. A. Bailie, R. P. Ley och A. Pasricha, "A Summary Review of Composite Laminate Design Guidelines," Northrop Grumman, El Segundo, California, 1997.
- [15] B. T. Åström, Manufacturing of Polymer Composites, Stockholm: Chapman & Hall, 1997.
- [16] A. Vicari, "Will Carbon Fiber Find Widespread Use in the Automotive Industry?," Machine Design, 2015. [Online]. Available: <http://machinedesign.com/contributing-technical-experts/will-carbon-fiber-find-widespread-use-automotive-industry>. [Accessed 18 06 2016].
- [17] R. N. Shama, T. G. A. Simha, K. P. Rao and R. Kumar, "Carbon Composites Are Becoming Competitive And Cost Effective," Infosys, 2015. [Online]. Available: <https://www.infosys.com/engineering-services/white-papers/Documents/carbon-composites-cost-effective.pdf>. [Accessed 10 02 2016].
- [18] Staff, "The Fiber," CompositesWorld, 2014. [Online]. Available: <http://www.compositesworld.com/articles/the-fiber>. [Accessed 6 04 2016].
- [19] "HexFlow RTM 6," Hexcel Composites, 2016. [Online]. Available: http://www.hexcel.com/Resources/DataSheets/RTM-Data-Sheets/RTM6_global.pdf. [Accessed 15 02 2016].
- [20] "Carbon Fiber Reinforced Pultrusions Technical Data Sheet," Creative Pultrusions, [Online]. Available: <http://www.creativepultrusions.com/index.cfm/products-solutions/custom-pultrusions/carbon-reinforced-pultrusions/>. [Accessed 15 02 2016].
- [21] "Henkel automotive molding process uses polyurethane in RTM," Composites World, 2013. [Online]. Available: <http://www.compositesworld.com/news/henkel-automotive-molding-process-uses-polyurethane-in-rtm>. [Accessed 17 02 2016].
- [22] Trailer, *Trailer Advertisement pp. 61*, Vimmerby: Trailer Magazine no. 2, 2016.
- [23] E. Lindström, "Utveckling av differentierade ersättningar för rundvirkestransporter med lastbil," Sveriges lantbruksuniversitet, Umeå, 2010.
- [24] "Egenskaper Hos Barrträ," Svenskt Trä, [Online]. Available: <http://www.svenskttra.se/om-tra/att-valja-tra/fran-timmer-till-planka/egenskaper-hos-barrtra/>. [Accessed 18 02 2016].
- [25] D. Zenkert and M. Battley, Foundations of Fibre Composites, Second Edition ed., vol. 2014, Stockholm: Royal Institute of Technology, 2003.
- [26] W. R. Broughton, L. E. Crocker och M. R. L. Gower, "Design Requirements for Bonded and Bolted Composite Structures," National Physical Laboratory, Teddington, Middlesex, 2002.

- [27] K. Potter, Introduction to Composite Products: Design, development and manufacture, Bristol: Springer Science & Business Media, 1996.
- [28] F. C. Campbell, Structural Composite Materials, ASM International, 2010.
- [29] T. Ireman, "Design of Composite Structures Containing Bolt Holes and Open Holes," Royal Institute of Technology, Stockholm, 1998.
- [30] J. Ekh, "Multi-Fastener Single-lap Joints in Composite Structures, Doctoral thesis," Royal Institute of Technology, Stockholm, 2006.
- [31] F.-K. Chang, R. A. Scott and S. G. Springer, "Strength of Mechanically Fastened Composite Joints," *Journal of Composite Materials*, vol. 16, pp. 470-494, 1982.
- [32] H. A. Withworth, O. Aluko and N. A. Thomson, "Application of the point stress criterion to the failure of composite pinned joints," *Engineering Fracture Mechanics*, vol. 75, pp. 1829-1839, 2008.
- [33] S. Yashiro, K. Ogi, T. Yamamoto and T. Watanabe, "A Simple Approach for Determining the Characteristic Distance in the Point Stress Criterion for Holed CFRP Unidirectional Laminates," *Advanced Composite Materials*, vol. 19, pp. 243-259, 2010.
- [34] K. -H. Tsai, C. -L. Hwan, M. -J. Lin och Y. S. Huang, "Finite Element Based Point Stress Criterion for Predicting the Notched Strengths of Composite Plates," *Journal of Mechanics*, vol. 28, nr 3, pp. 401-406, 2012.
- [35] C. T. Sun, B. J. Quinn, J. Tao och D. W. Oplinger, "COMPARATIVE EVALUATION OF FAILURE ANALYSIS METHODS FOR COMPOSITE LAMINATES," U.S. Department of Transportation Federal Aviation Administration, Washington, 1996.
- [36] S. E. Yamada and C. T. Sun, "Analysis of Laminate Strength and Its Distribution," *Journal of Composite Materials*, vol. 12, pp. 275-284, 1978.
- [37] G. Perillo, N. P. Vedvik och A. T. Echtermeyer, "Numerical application of three-dimensional failure criteria for laminated composite materials," Providence, Rhode Island, 2010.
- [38] A. Puck and H. Schurmann, "Failure analysis of FRP laminates by means of physically based phenomenological models," *Composites Science and Technology* 62 (2002) 1633–1662, vol. 62, pp. 1633-1662, 2002.
- [39] A. Puck, J. Kopp and M. Knops, "Guidelines for the determination of the parameters in Puck's action plane strength criterion," *Composites Science and Technology*, vol. 62, pp. 371-378, 2002.
- [40] R. G. Cuntze and A. Freund, "The predictive capability of failure mode concept-based strength criteria for multidirectional laminates," *Composites Science and Technology*, vol. 64, pp. 343-377, 2004.

- [41] M. J. Hinton, P. D. Soden and A. S. Kaddour, "Recommendations for designers and researchers resulting from the world-wide failure exercise," in *Failure Criteria in Fibre Reinforced Polymer Composites*, Elsevier Science Ltd, 2004, pp. 1223-1251.
- [42] Simulia, "Getting Started with Abaqus: Interactive Edition, Ch. 9," Simulia.
- [43] T. Jollivet, C. Peyrac and F. Lefebvre, "Damage of Composite Materials," *Procedia Engineering*, pp. 1-13, 2013.
- [44] K. Dreschler, M. Heine, P. Mitschang, W. Baur, U. Gruber, L. Fischer, O. Öttinger, B. Heidenreich, N. Lutzenburger och H. Vögenreiter, "Carbon fiber Reinforced Composites," *Ullmans encyclopedia of industrial chemistry*, pp. 18-19, 2009.
- [45] T. Nyman, "Composite fatigue design methodology: a simplified approach," *Composite Structures*, vol. 35, pp. 183-194, 1996.
- [46] N. T. Phong, M. H. Gabr, L. H. Anh, V. M. Duc, A. Betti, K. Okubo, B. Chuong och T. Fujii, ". Improved fracture toughness and fatigue life of carbon fiber reinforced epoxy composite due to incorporation of rubber nanoparticles," *Journal of Material Science*, vol. 48, pp. 6039-6047, 2013.

Appendix A. Fatigue of fibre composites

Many of the structures in the automotive and transport industry are designed to last several years and during a high number of load cycles. This implies high demands on the fatigue properties of the components.. A ratio used for comparing and analysing fatigue life of composites is the fatigue load ratio

$$R_{fat} = \frac{\sigma}{\hat{\sigma}} \quad (A.1)$$

for a given number of cycles. R_{fat} is the load ratio between calculated stress σ in the structure and the static strength limit $\hat{\sigma}$. Depending on material data the ratio can vary but in general crack growth is avoided if the ratio is below 0.6 [43]. For example a fatigue load ratio of 0.6 is indicated for a CFRP to withstand 10^6 load cycles, [44]. In “Damage of composite materials” [43] fatigue load ratios between 0.5 and 0.7 can be seen. The scatter in fatigue load ratio highlights the importance of material combination and layup. Designing against fatigue of fibre composites is done within this report by the use of a simplified design criterion, namely by using a safety factor of 3 against ultimate static strength, i.e. $R_{fat} = 1/3$.

Guidelines based solely on a fatigue load ratio is a simplification that has to be used with caution. To further validate a fatigue load ratio dependent criterion one has to recall that fibre composite has different fatigue properties in tension and compression. An analysis based solely on R_{fat} does not consider the load ratio,

$$R = \frac{\sigma_{min}}{\sigma_{max}}. \quad (A.2)$$

The difference between compression and tension is exemplified by a numerical example in [43] where its seen that the fatigue load ratio decreases significantly between a tensile-tensile and tensile-compression load cycle. A test has also been performed with constant amplitude and varying R values confirming the decreased fatigue properties of the composite when loading in compression [45]. The experimental results from Nyman [45] indicates fatigue load ratios similar to previously mentioned values even though a strain failure criterion is used in contrast to previous stress based comparisons. In summary these investigations indicate that a safety factor of 3 against static strength is a reasonable assumption.

Appendix B. Material properties

During the FE-analysis of the timber bolster the material data in Table B.1 was used.

Table B.1: *Material properties [25].*

Property	Carbon-epoxy	Glass-epoxy
ρ [kg/m ³]	1610	1940
E_1 [GPa]	151	40
E_2 [GPa]	9.4	9.8
G_{12} [GPa]	4.8	2.8
$\hat{\sigma}_{1t}$ [MPa]	2260	1100
$\hat{\sigma}_{1c}$ [MPa]	1200	600
$\hat{\sigma}_{2t}$ [MPa]	50	20
$\hat{\sigma}_{2c}$ [MPa]	190	140
\hat{t}_{12} [MPa]	100	70
\hat{t}_{23} [MPa]	100	-
\hat{t}_{13} [MPa]	100	-
$\hat{\epsilon}_{1t}$	0.015	0.028
$\hat{\epsilon}_{1c}$	0.008	0.015
$\hat{\epsilon}_{2t}$	0.005	0.002
$\hat{\epsilon}_{2c}$	0.02	0.014
$\hat{\gamma}_{12}$	0.022	0.014

Appendix C. Rubber epoxy

There are several ways one can lower the risk of failure in composites. A method that lowers the risk of fracture and increases the fatigue life is to add rubber particles into the epoxy resin [46]. The rubber particles were of 35 nm in size. The presented results were done comparing 3, 5 and 8 weight percentage of rubber within the epoxy-matrix. The addition of rubber particles significantly improved the carbon fibre epoxy composites mechanical properties. More specifically fracture toughness, tensile strength and fatigue life was tested. The fracture toughness increased with the percentage of rubber, however the biggest improvement occurred when going from 0 to 3% of rubber. The same reference [46] also provides results indicating that the tensile strength is increased by using rubber particles within the epoxy resin. On the other hand a slight decrease in Young's modulus was observed when analysing rubber modified carbon-epoxy composites [46]. A significant improvement in the fatigue life was observed. The number of cycles to failure increased by up to a factor of 100 [46]. The fatigue tests were performed for different stress levels with a load ratio of 0.1. For all tests, with and without modified epoxy the number of cycles ranged from 500 to 10 000 000.

Appendix D. Optimisation layup of non-design space

The layup of the non-design space of the optimised timber bolster is displayed in Table D.1. Note that due to symmetry only half of the layup is displayed.

Table D.1: *Layup for non-design space in optimisation procedure.*

Material	Thickness [mm]	Fibre orientation [°]
Glass	0.5	-45
Glass	0.5	45
Carbon	0.25	-45
Carbon	0.25	45
Carbon	0.25	0
Carbon	0.25	0
Carbon	0.25	-45
Carbon	0.25	45
Carbon	0.25	90
Carbon	0.25	0
Carbon	0.25	-45
Carbon	0.25	45
Carbon	0.25	0
Carbon	0.25	0
Carbon	0.25	-45
Carbon	0.25	45
Carbon	0.25	90
Carbon	0.25	0
Carbon	0.25	-45
Carbon	0.25	45
Carbon	0.25	0
Carbon	0.25	0
Carbon	0.25	-45
Carbon	0.25	45
Carbon	0.25	90
Carbon	0.25	0

Appendix E. Optimised ply shapes

Optimised ply shapes used for the 0° fibre orientation are displayed in Figure E.1 below and corresponding for the other fibre orientations in Figure E.2 below.

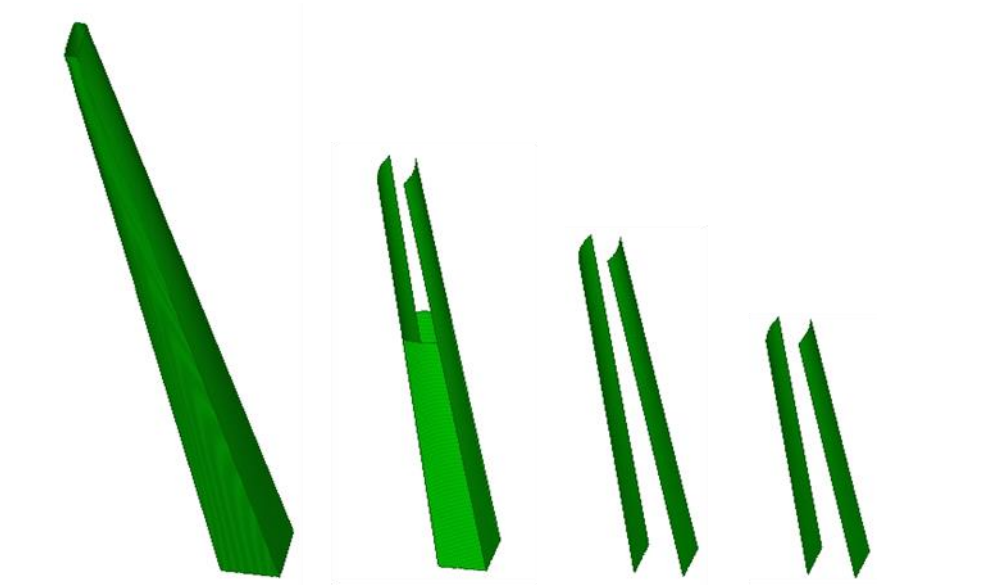


Figure E.1: *Ply shapes used for 0° fibre orientation.*

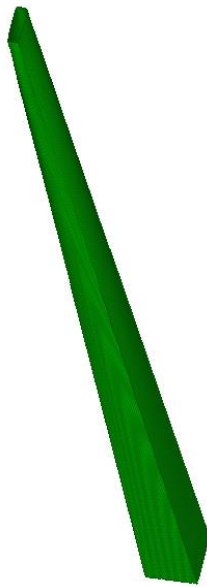


Figure E.2: *Ply shape used for 90° , 45° and -45° orientation.*

Appendix F. Maximum strain variation

The variation of the maximum strain criterion when the optimised structure is subjected to the $0.3g \cdot 10$ tonnes bending load on the vertical beam is displayed in in Figure F.1.

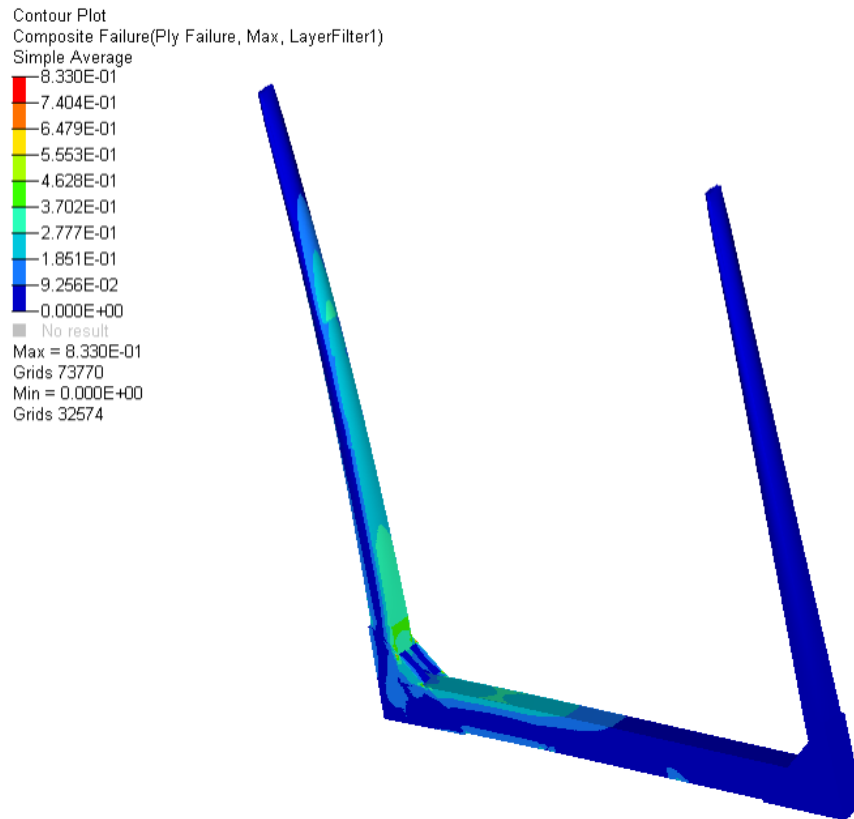


Figure F.1: *Contour plot of maximum strain criterion for carbon fibre layers.*

Appendix G. Abaqus UMAT subroutine

The following appendix presents the Abaqus subroutine for evaluation of the composite failure in the bolt analysis. The subroutine is called from the Abaqus input file in the material definition with the USER MATERIAL command, for example

```
*MATERIAL, NAME=carbonIM_solid
*DENSITY
1610.0, 0.0
*USER MATERIAL, CONSTANTS = 9
1.5100E+11, 9.4000E+09, 9.4000E+09, 0.31, 0.31, 0.5, 4.8000E+09, 4.8000E+09
4.8000E+09, 0.0
*DEPVAR
1,
```

The output of the subroutine is defined as a state variable in the output definition as follows

```
*OUTPUT, FIELD, FREQUENCY = 1
*ELEMENT OUTPUT
SDV1
```

The following presents the Abaqus UMAT subroutine for the Yamada-Sun failure criterion. The other failure criteria are defined similarly. The subroutine defines the complete mechanical response of the composite material.

```
SUBROUTINE UMAT(stress,statev,ddsdde,sse,spd,scd,
1 rp1,ddsddt,drplde,drpldt,
2 stran,dstran,time,dtime,temp,dtemp,predef,dpred,cmname,
3 ndi,nshr,ntens,nstatv,props,nprops,coords,drot,pnewdt,
4 celent,dfgrd0,dfgrd1,noel,npt,layer,kspt,kstep,kinc)

INCLUDE 'ABA_PARAM.INC'

CHARACTER*80 CMNAME

DIMENSION stress(ntens),statev(nstatv),
1 ddsdde(ntens,ntens),ddsddt(ntens),
2 drplde(ntens),stran(ntens),dstran(ntens),
3 time(2),predef(1),dpred(1),props(nprops),
4 coords(3),drot(3,3),dfgrd0(3,3),dfgrd1(3,3)

DIMENSION C(ntens,ntens),dstress(ntens)

PARAMETER (zero=0.d0,one=1.d0,two=2.d0,three=3.d0,four=4.d0,
1 NintyProc=0.9d0, OneP=0.01d0, half=0.5d0,
2 XT=2260D6, XC=1200D6, YT=50D6, YC=190D6,
3 Sst=100D6)

C check for consistency between the specified and
C required number of input parameters
C-----

if (nprops.ne.9) then
write(*,*) '** error : this umat requires 9 param'
stop
endif

C save props to stiffness variables
C-----
E11 = props(1)
E22 = props(2)
E33 = props(3)
v12 = props(4)
v13 = props(5)
v23 = props(6)
```

```

G12 = props(7)
G13 = props(8)
G23 = props(9)
v21 = (v12/E11)*E22
v32 = (v23/E22)*E33
v31 = (v13/E11)*E33

```

C material stiffness matrix definition ORTHOTROPIC MATERIAL

C-----

```

del = (1-v12*v21-v23*v32-v31*v13-2*v21*v32*v13)/(E11*E22*E33)

```

```

C(1,1)= (1-v23*v32)/(E22*E33*del)
C(1,2)= (v21+v31*v23)/(E22*E33*del)
C(1,3)= (v31+v21*v32)/(E22*E33*del)
C(1,4)= zero
C(1,5)= zero
C(1,6)= zero
C(2,1)= (v21+v31*v23)/(E22*E33*del)
C(2,2)= (1-v13*v31)/(E11*E33*del)
C(2,3)= (v32+v12*v31)/(E11*E33*del)
C(2,4)= zero
C(2,5)= zero
C(2,6)= zero
C(3,1)= (v31+v21*v32)/(E22*E33*del)
C(3,2)= (v32+v12*v31)/(E11*E33*del)
C(3,3)= (1-v12*v21)/(E11*E22*del)
C(3,4)= zero
C(3,5)= zero
C(3,6)= zero
C(4,1)= zero
C(4,2)= zero
C(4,3)= zero
C(4,4)= G23
C(4,5)= zero
C(4,6)= zero
C(5,1)= zero
C(5,2)= zero
C(5,3)= zero
C(5,4)= zero
C(5,5)= G31
C(5,6)= zero
C(6,1)= zero
C(6,2)= zero
C(6,3)= zero
C(6,4)= zero
C(6,5)= zero
C(6,6)= G12

```

C calculate the current stress incrementss

C-----

C Product of stiffness matrix and strain matrix

C This UMAT is meant to be used with solid elements, and would have 3 ndi terms, and 3 nshr terms

```

do k1=1,ndi
  term1=zero
  term2=zero
  do k2=1,ndi
    term1=term1+C(k1,k2)*dstran(k2)
    term2=term2+C(k1,k2)*(dstran(k2)+stran(k2))
  end do

  dstress(k1)=term1
  stress(k1)=term2
end do

```

C This UMAT is meant to be used with solid elements, and would have 3 ndi terms, and 3 nshr terms

C The stress terms corres tp nshr terms 1,2,3 would be 4,5,6 respectively

```

do k1=1,nshr
  dstress(k1+ndi)=C(k1+ndi,k1+ndi)*dstran(k1+ndi)
  stress(k1+ndi)=C(k1+ndi,k1+ndi)*(dstran(k1+ndi)+stran(k1+ndi))
end do

C          YAMADA-SUN failure criterion

t12 = stress(4)
if (stress(1).ge.zero) then
  sig_max_1 = XT
else
  sig_max_1 = XC
end if
YSun2 = (stress(1)/sig_max_1)**two+(t12/Sst)**two
YSun = sqrt(YSun2)
statev(1)=YSun

C -----create jacobian matrix-----
do k1=1,ntens
  do k2=1,ntens
    ddsdde(k2,k1)=zero
  end do
end do

do k1=1,ndi
  ddsdde(k1,k1)=C(k1,k1)
end do

do k1=2,ndi
  n2=k1-1
  do k2=1,n2
    ddsdde(k2,k1)=C(k2,k1)
    ddsdde(k1,k2)=C(k1,k2)
  end do
end do

i1=ndi
do k1=1,nshr
  i1=i1+1
  ddsdde(i1,i1)=C(i1,i1)
end do

C specific elastic energy
C-----
tde=zero
do k1=1,ntens
  tde=tde+(stress(k1)+0.5*dstress(k1))*dstran(k1)
end do

dee=zero
do k1=1,ndi
  term1=zero
  term2=zero
  do k2=1,ndi
    term1=term1+C(k1,k2)*stran(k2)
    term2=term2+C(k1,k2)*dstran(k2)
  end do
  dee=dee+(term1+half*term2)*dstran(k1)
end do

i1=ndi
do k1=1,nshr
  i1=i1+1
  dee=dee+C(i1,i1)*(stran(i1)+half*dstran(i1))*dstran(i1)
end do
sse=sse+dee

return
end

```